View metadata, citation and similar papers at core.ac.uk

brought to you by CORE

İSTANBUL TECHNICAL UNIVERSITY ★ INSTITUTE OF SCIENCE AND TECHNOLOGY

THE USE OF THIN LAYER CONDITIONS TO RECONSTRUCT OBJECTS BURIED IN A LAYERED MEDIUM

M.Sc. Thesis by
Alaaddin YAKA

Department : Electronics and Communication Engineering

Programme : Telecommunication Engineering

JUNE 2010

İSTANBUL TECHNICAL UNIVERSITY ★ INSTITUTE OF SCIENCE AND TECHNOLOGY

THE USE OF THIN LAYER CONDITIONS TO RECONSTRUCT OBJECTS BURIED IN A LAYERED MEDIUM

M.Sc. Thesis by
Alaaddin YAKA
(504081301)

Date of submission : 07 May 2010
Date of defence examination : 07 June 2010

Supervisor (Chairman) : Assis. Prof. Dr. Özgür ÖZDEMİR (ITU)
Members of the Examining Committee : Assoc. Prof. Dr. Ali YAPAR (ITU)
Assis. Prof. Dr. Semra AHMETOLAN (ITU)

JUNE 2010

İSTANBUL TEKNİK ÜNİVERSİTESİ ★ FEN BİLİMLERİ ENSTİTÜSÜ

TABAKALI BİR ORTAMDA GÖMÜLÜ CİSİMLERİN GÖRÜNTÜLENMESİNDE İNCE TABAKA KOŞULLARININ KULLANILMASI

YÜKSEK LİSANS TEZİ
Alaaddin YAKA
(504081301)

Tezin Enstitüye Verildiği Tarih : 07 Mayıs 2010
Tezin Savunulduğu Tarih : 07 Haziran 2010

Tez Danışmanı : Yrd.Doç. Dr. Özgür ÖZDEMİR (İTÜ)
Diğer Jüri Üyeleri : Doç. Dr. Ali YAPAR (İTÜ)
Yrd. Doç. Dr. Semra AHMETOLAN (İTÜ)

HAZİRAN 2010

FOREWORD

I would like to express my appreciation and thanks for my advisor Assis. Prof. Dr. Özgür Özdemir, who gave me the opportunity to work under her supervision.

I would like to thank to my family for their endless support.

Finally, I would like to thank to TUBITAK (The Scientific and Technological Research Council of Turkey) for supporting me financially by the fellowship programme 2210.

June 2010

Alaaddin YAKA

Telecommunication Engineer

TABLE OF CONTENTS

Page

ABBREVIATIONS

RG-LSM **:** Reciprocity Gap Linear Sampling Method
PEC **:** Perfect Electric Conductor
TLC : Thin Layer Condition
TM **:** Transverse Magnetic

LIST OF FIGURES

Page

THE USE OF THIN LAYER CONDITIONS TO RECONSTRUCT OBJECTS BURIED IN A LAYERED MEDIUM

SUMMARY

In this thesis, one of the generalized boundary conditions which are called Thin Layer Conditions (TLC) are extended to the rough interfaced thin layers. With these conditions, fields values can be calculated without knowledge of background Green function which is not available analytically for rough interfaced layered medium. Then Thin Layer Conditions are combined with Reciprocity Gap-Linear Sampling Method (RG-LSM) to reconstruct buried objects under multi-layered medium.

At the first part of the thesis, Thin Layer Conditions are derived for layered medium having rough interface. For this purpose, first Helmholtz equation is written in curvilinear coordinates and then asymptotic expansion of the total field inside the layer are done in terms of the thickness of the layer. Applying boundary conditions at the upper and bottom boundary of the layer, the field values at the bottom layer are determined in term of the field values at the upper layer and by rearranging them, TLC can be written in well-known boundary condition format. The number of terms of in truncated asymptotic series determines the accuracy and/or order the TLC. In this thesis, TLCs up to fourth order are derived. Moreover, we have also proposed Cascaded TLC to improve accuracy of approximation of field.

The second part of the thesis is concerned with detection of buried object under multi-layered medium and RG-LSM method is employed for this aim. In this thesis, we have chosen the RG-LSM method for solution of inverse scattering problem since it does not need to know Green function of the background medium, it only needs field and its normal derivative on the interface which covers the medium which is objects buried. With TLC, the data for RG-LSM are easily obtained for many layers which are flat or rough interfaced. Another reason for choosing RG-LSM is that it makes possible reconstruction without any restriction and any priori knowledge about physical and geometrical properties of the buried object.

TABAKALI BİR ORTAMDA GÖMÜLÜ CİSİMLERİN GÖRÜNTÜLENMESİNDE İNCE TABAKA KOŞULLARININ KULLANILMASI

ÖZET

Bu tezde, ilk olarak genelleştirilmiş sınır koşullarından biri olan ince tabaka koşulları, pürüzlü arayüzlü ince tabakalara genişletilmiştir. Bu koşullarla, alan değerleri Green fonksiyonu bilgisi olmadan hesaplanabilir, ki bu fonksiyon pürüzlü arayüzlü tabakalı ortamlar için analitik olarak hesaplanamaz. Daha sonra ise, ince tabaka koşulları RG-LSM ile birleştirilerek çok tabakalı ortamda gömülü cisimlerin görüntülenmesi problemi ele alınmıştır.

Tezin ilk kısmında, pürüzlü arayüze sahip tabakalı ortamlar için ince tabaka koşulları elde edilmiştir. Bu amaçla, ilk olarak Helmholtz denklemi eğrisel koordinatlarda yazılmış ve tabakanın içindeki toplam alanın tabakanın kalınlığı cinsinden asimptotik açılımı yapılmıştır. Tabakanın üst ve alt sınırlarında, sınır koşullarını uygulayarak, alt tabakadaki alan değerleri, üst tabakadaki alan değerleri cinsinden belirlenir ve bunlar yeniden düzenlenerek, ince tabaka koşulları bilinen klasik sınır koşulları biçiminde yazılabilir. Asimptotik seride alınan terimlerin sayısı, ince tabaka koşullarının doğruluğunu ve/veya derecesini belirler. Bu tezde, 4. dereceye kadar olan ince tabaka koşulları hesaplanmıştır. Buna ek olarak, alan yaklaşıklığının doğruluğunu artırmak için kaskat ince tabaka koşulları önerilmiştir.

Tezin ikinci kısmında, çok tabakalı ortamda gömülü cisimlerin görüntülenmesi problemi RG-LSM ile çözülmüştür. RG-LSM'nin seçilmesinin sebebi, yöntemin ortamın Green fonksiyonuna ihtiyaç duymamasıdır. Burada sadece gömülü nesnenin bulunduğu ortamı çevreleyen arayüzey üzerindeki alan ve alanın normal türevi değerleri kullanılır. RG-LSM için kullanılacak bu veriler, İnce tabaka koşulları yardımıyla çok tabakalı düz veya pürüzlü arayüzeyler için kolaylıkla bulunur. RG-LSM'nin sağladığı diğer bir avantaj ise gömülü nesnenin fiziksel veya geometriksel özellikleri hakkında herhangi bir ön bilgi veya herhangi bir sınırlama gerektirmemesidir.

1. INTRODUCTION

Equivalent boundary conditions are widely used for mathematical modeling in the solution of scattering problems [1-11]. Here the main idea to use equivalent boundary conditions is to replace the complex scattering problem with one having new boundary conditions which can be solved in a more easier way than the original one. These conditions are important in all disciplines, e.g. acoustics, hydrodynamics and electromagnetics, where boundary conditions are involved. In electromagnetics, equivalent boundary conditions are especially used for modeling of geometrical and physical properties of the actual structure in scattering, propagation and antenna problems. The simplest equivalent boundary conditions are the standard impedance conditions applicable at the surface of a lossy dielectric, and the related transition conditions which model a thin dielectric layer as a current sheet[2-6]. Although these have been available for many years that the impedance boundary condition came into use in connection with ground wave propagation over the earth. As a result of impedance boundary conditions' simplicity, ease of use and successful application, improved or higher order versions of the impedance boundary conditions are now being considered for electromagnetic applications. These higher order impedance boundary conditions, often referred to as generalized impedance boundary conditions, permit the simulation of more complicated material and composite surfaces with greater accuracy.

When Equivalent boundary conditions are used to model thin layers, they are called as ***Thin Layer Conditions*** [7-11]. Such conditions connect the fields only on the boundaries of the slab or even on some effective surfaces, so that the field distribution inside the layer is no longer necessary to be considered. The problem with two different media can thus be converted into a problem with single medium and complex boundary conditions. The importance of this arises from the efforts of reducing the computational constraints due to the thin layer. Computing without the need to directly resolve the thin layer significantly reduces the size of the discrete model and consequently reduces the computations, especially when the thin layer is thin compared to the wavelength of the incident wave.

These conditions are very important for practical application in which layered medium is involved, such as geophysics, underground imaging, etc. Even though there are many studies in the literature, most of them are dealing with thin layer with flat interface. However, usually interfaces are not flat and assuming them as flat might lead a wrong result. Here, in this thesis, we have developed higher order generalized thin layer conditions which are valid for both rough and flat interface. To this aim, we use curvilinear coordinates and Helmholtz equation and all the related boundary conditions are written in curvilinear coordinates. Then, the field in the thin layer is expanded into a asymptotic series in terms of its thickness and thin layer conditions are obtained by using boundary conditions at the upper and lower interface of the layer. The order of thin layer conditions is determined by the number of term in truncated asymptotic series. In this work, we derived the TLC up to fourth order.

On the other hand, reconstruction of objects buried in layered medium has been very popular subject in many areas and constitutes an inverse scattering problem. They have very important practical applications such as mine detection, tumor cells recognition, through wall surveillance, etc. The capability of retrieving the geometrical features of a system of unknown targets from the measures of the scattered fields is also important in many non-invasive diagnostics applications.

Several techniques have been developed to image buried objects such as contrast source inversion method [12,13], Born iterative method/Distorted Born iterative method [14,15], linear sampling type methods [16-19] and other inversion algorithms[20-28]. Most of these methods need to know Green function of background medium which is not available analytically for rough interface. One need to assume that interface is flat to be able to use these algorithms. Besides, these methods are applicable only metallic or dielectric objects, hence, even before detection, knowledge of the characteristics of the object is necessary.

Among these methods, linear sampling type methods do not require any priori knowledge of the physical and geometrical properties of the scattering object, but still needs the Green function of the background medium. However, recently Reciprocity Gap Linear Sampling Method (RG-LSM), combination of the ideas of the linear sampling method and the use of the reciprocity gap functional is proposed to overcome this drawback [29-32]. To be able to use RG-LSM, we need to know the field value and its normal derivative on the boundary of the medium which the object is located.

In this thesis, we consider that objects are buried under a multi-layered medium with flat and rough interface. From measurement of the field and its normal derivative at the top interface of the medium, we implement thin layer conditions to obtain the field values at the lowest interface which covers the medium where object is placed. Then, we apply the RG-LSM to detect shape and localization of the object.

In section 2, thin layer conditions are derived up to fourth order in the differential form for general interface type and solution method of this differential equation is explained. Then in section 3, overview of RG-LSM is given. Finally numerical results are presented to show the applicability of the proposed method in section 4, for planar medium with flat and rough interface and cylindrical medium with circular interface.

2. THIN LAYER CONDITIONS

Equivalent boundary conditions are called as Thin Layer Conditions when they are used for modeling thin layers. Thin Layer conditions provide an equation which link the field and the normal derivative of the field at the upper boundary of the thin layer to the field and the normal derivative of field at the lower boundary of the thin layer.

Therefore, there is no need to solve Helmholtz equation inside the thin layer. The only requirement is that in the region of interest the field obtained using the postulated condition approximates the exact field to an adequate degree of accuracy. One of the advantage of this, multi-layered structures with ordinary boundary conditions can be thought as two-layered medium with thin layer conditions on it. Thus, especially numerical cost of inverse scattering problems can be reduced in this way.

In this section, we first give the outline of derivation of the higher order thin layer conditions up to 4th order. Then we will explain how to solve these differential equation systems.

2.1 Derivation of Generalized Thin Layer Conditions

Let's consider a thin layer (Ω^δ) of thickness of δ in the domain Ω. Let $\partial\Omega_+{}^\delta$, and $\partial\Omega_-{}^\delta$ be the outer and inner boundary of the thin layer, respectively and Γ be defined as $\Gamma = \frac{1}{2}\left(\partial\Omega_+{}^\delta + \partial\Omega_-{}^\delta\right)$, i.e., the parallel interface located half way between the two boundaries (see Fig. 2.1.). Note when normal vector $\vec{n}$ is given on Γ, the outer and inner boundaries of Ω^δ can be expressed as $\Gamma \pm (\frac{\delta}{2})\vec{n}$.

The comprehensive equations in whole space for this given configuration are

$$\begin{cases} \Delta\tilde{u}^\delta + k^2\tilde{u}^\delta = 0 & R^2\backslash\Omega^\delta \\ \Delta u^\delta + k^2 u^\delta = 0 & \Omega^\delta \end{cases} \tag{2.1}$$

and the boundary conditions which belong to tangential components on $\partial\Omega_-^\delta$ and $\partial\Omega_+^\delta$ for TM polarization $\left(H_z = 0, E_z = (0,0,u)\right)$ are

$$\begin{cases} \tilde{u}^{\delta}(x) = u^{\delta}(x) \\ \frac{\partial \tilde{u}^{\delta}}{\partial n}(x) = \frac{\partial u^{\delta}}{\partial n}(x) \end{cases} \quad \textbf{(2.2)}$$

Using the above equalities, the equations (2.1) can be expressed as in curvilinear coordinates (s, υ) where $\upsilon = \delta\xi$

$$\frac{1}{(1+\delta\xi C)}\frac{\partial}{\partial s}\frac{1}{(1+\delta\xi C)}\frac{\partial}{\partial s}u + \frac{1}{\delta^2}\frac{1}{(1+\delta\xi C)}\frac{\partial}{\partial \xi}(1+\delta\xi C)\frac{\partial}{\partial \xi}u + k^2 u = 0 \quad \textbf{(2.3)}$$

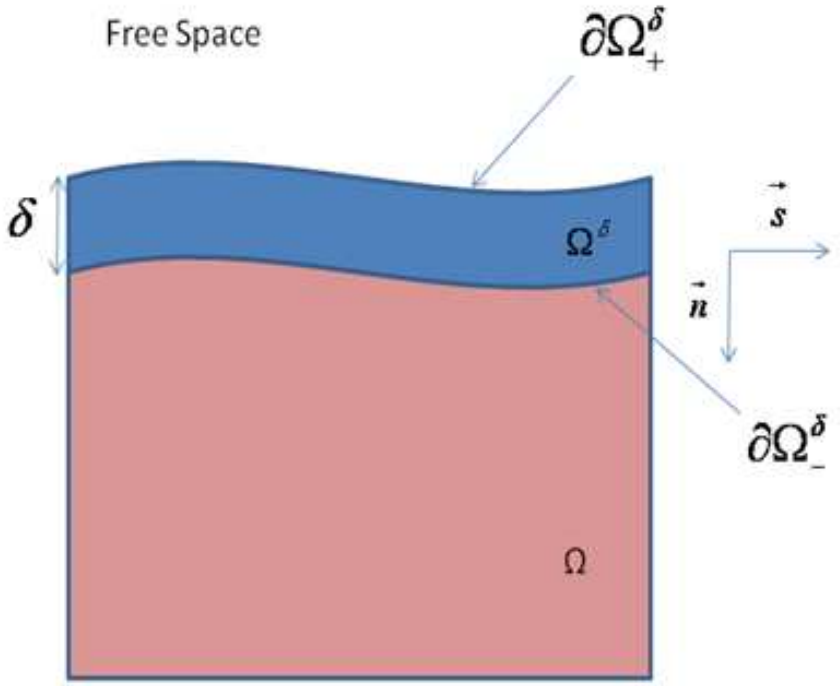

Figure 2.1 : Notation for boundaries and domains.

In (2.3), the term C symbolizes curvature. If we multiply both sides of the equations (2.1) with $(1+\delta\xi C)^3$, (2.1) can be expressed as follows,

$$\begin{aligned}(1+\delta\xi C)^3\,\Delta + (1+\delta\xi C)^3\,k^2 = {} & \frac{1}{\delta^2}\frac{\partial^2 u}{\partial \xi^2} \\ & + \frac{1}{\delta}\left(\mathrm{C}\,\frac{\partial u}{\partial \xi} + 3\xi\mathrm{C}\frac{\partial^2 u}{\partial \xi^2}\right) \\ & + \left(\left(\frac{\partial^2 u}{\partial s^2} + 2\xi C^2\frac{\partial u}{\partial \xi} + 3(\xi C)^2\frac{\partial^2 u}{\partial \xi^2}\right) + k^2 u\right) \\ & + \delta\left(\left(\xi\mathrm{C}\,\frac{\partial^2 u}{\partial s^2} - \xi C'\frac{\partial u}{\partial s} + \xi^2 C^3\frac{\partial u}{\partial \xi} + \xi^3 C^3\frac{\partial^2 u}{\partial \xi^2}\right) + 3\xi\mathrm{C}k^2 u\right) \\ & + \delta^2(3\xi^2 C^2 k^2)u \\ & + \delta^3(\xi^3 C^3 k^2)u \end{aligned} \quad \textbf{(2.4)}$$

To compute the generalized thin layer conditions, asymptotic expansion is applied to u and $\frac{\partial u}{\partial n}$.

$$u = u_0 + \delta u_1 + \delta^2 u_2 + \delta^3 u_3 + \ ... \quad \textbf{(2.5)}$$

$$\frac{\partial u}{\partial n} = \frac{\partial u_0}{\partial n} + \delta \frac{\partial u_1}{\partial n} + \delta^2 \frac{\partial u_2}{\partial n} + \delta^3 \frac{\partial u_3}{\partial n} + \ ... \quad \textbf{(2.6)}$$

If we want to derive $(\boldsymbol{k+1})^{\boldsymbol{th}}$ order conditions, we have to include $\boldsymbol{\delta^k}$ order terms in asymptotic expansion.

If we rewrite the (2.4), using (2.5) and (2.6),

$$\frac{\partial^2 U_j}{\partial \xi^2} = -B_1\, u_{j-1} - B_2 u_{j-2} - B_3 u_{j-3} - B_4 u_{j-4} - B_5 u_{j-5} \quad \textbf{(2.7)}$$

where $B_1 = \left(\mathrm{C}\,\frac{\partial}{\partial \xi} + 3\xi \mathrm{C}\frac{\partial^2}{\partial \xi^2}\right)$, $B_2 = \left(\left(\frac{\partial^2}{\partial s^2} + 2\xi C^2 \frac{\partial}{\partial \xi} + 3(\xi C)^2 \frac{\partial^2}{\partial \xi^2}\right) + k^2\right)$,

$B_3 = \left(\left(\xi \mathrm{C}\,\frac{\partial^2}{\partial s^2} - \xi C' \frac{\partial}{\partial s} + \xi^2 C^3 \frac{\partial}{\partial \xi} + \xi^3 C^3 \frac{\partial^2}{\partial \xi^2}\right) + 3\xi \mathrm{C} k^2\right)$, $B_4 = (3\xi^2 C^2 k^2)$,

and $B_5 = (\xi^3 C^3 k^2)$.

To derive the higher order thin layer conditions, we use the procedure given below:

$$\upsilon(s,\xi) = <\upsilon> + \frac{1}{2}\left(\int_{-\frac{1}{2}}^{\xi} \frac{\partial}{\partial \xi}\upsilon - \int_{\xi}^{\frac{1}{2}} \frac{\partial}{\partial \xi}\upsilon\right) \quad \textbf{(2.8)}$$

$$[\upsilon] = \int_{-\frac{1}{2}}^{\frac{1}{2}} \frac{\partial}{\partial \xi}\upsilon \, d\xi \quad \textbf{(2.9)}$$

$$\frac{\partial}{\partial \xi}\upsilon(s,\xi) = <\frac{\partial \upsilon}{\partial \xi}> + \frac{1}{2}\left(\int_{-\frac{1}{2}}^{\xi} \frac{\partial^2 \upsilon}{\partial \xi^2} - \int_{\xi}^{\frac{1}{2}} \frac{\partial^2 \upsilon}{\partial \xi^2}\right) \quad \textbf{(2.10)}$$

$$[\frac{\partial \upsilon}{\partial \xi}] = \int_{-\frac{1}{2}}^{\frac{1}{2}} \frac{\partial^2 \upsilon}{\partial \xi^2} \, d\xi \quad \textbf{(2.11)}$$

where $\upsilon^+ = \upsilon/\xi = \delta/2$, $\upsilon^- = \upsilon/\xi = -\delta/2$, $[\upsilon] = \upsilon^+ - \upsilon^-$ and $<\upsilon> = \frac{\upsilon^+ + \upsilon^-}{2}$.

Computation of higher order thin layer conditions procedure starts with (2.11), then (2.10),(2.9) and (2.8) are computed, respectively.

The procedure obtaining the zero order thin layer conditions as follows:

$$\frac{\partial^2 U_0}{\partial \xi^2} = 0 \quad \textbf{(2.12)}$$

$$\frac{\partial U_0}{\partial \xi}\left(\xi = \mp\frac{1}{2}\right) = 0 \quad \textbf{(2.13)}$$

$$[\frac{\partial U_0}{\partial \xi}] = 0 \quad \textbf{(2.14)}$$

$$\frac{\partial U_0}{\partial \xi}(s,\xi) = <\frac{\partial U_0}{\partial \xi}> \quad \textbf{(2.15)}$$

$$[U_0] = <\frac{\partial U_0}{\partial \xi}> \quad \textbf{(2.16)}$$

$$U_0 = <U_0> + \xi<\frac{\partial U_0}{\partial \xi}> \quad \textbf{(2.17)}$$

The computations to evaluate 1^{st} order thin layer conditions as follows:

$$\frac{\partial^2 U_1}{\partial \xi^2} = -(C\frac{\partial U_0}{\partial \xi} + 3\xi C\frac{\partial^2 U_0}{\partial \xi^2}) \quad \textbf{(2.18)}$$

$$[\frac{\partial U_1}{\partial \xi}] = -C<\frac{\partial U_0}{\partial \xi}> \quad \textbf{(2.19)}$$

$$\frac{\partial U_1}{\partial \xi} = <\frac{\partial U_1}{\partial \xi}> - C\xi <\frac{\partial U_0}{\partial \xi}> \quad \textbf{(2.20)}$$

$$[U_1] = <\frac{\partial U_1}{\partial \xi}> \quad \textbf{(2.21)}$$

$$U_1 = <U_1> - \frac{C}{2}(\xi - \frac{1}{2})(\xi + \frac{1}{2})<\frac{\partial U_0}{\partial \xi}> + \xi<\frac{\partial U_1}{\partial \xi}> \quad \textbf{(2.22)}$$

The numerical process to get 2^{nd} order thin layer conditions as follows:

$$\frac{\partial^2 U_2}{\partial \xi^2} = -(C\frac{\partial}{\partial \xi}U_1 + 3\xi C\frac{\partial^2 U_1}{\partial \xi^2}) - (\frac{\partial^2}{\partial s^2} + k^2 + 2\xi C^2\frac{\partial}{\partial \xi} + 3(\xi C)^2\frac{\partial^2}{\partial \xi^2})U_0 \quad \textbf{(2.23)}$$

$$\frac{\partial^2 U_2}{\partial \xi^2} = -C<\frac{\partial U_1}{\partial \xi}> + C^2\xi<\frac{\partial U_0}{\partial \xi}> + 3\xi C^2<\frac{\partial U_0}{\partial \xi}> - (\frac{\partial^2}{\partial s^2} + k^2)(<U_0> + \xi<\frac{\partial U_0}{\partial \xi}>)$$

$$-2\xi C^2<\frac{\partial U_0}{\partial \xi}> \quad \textbf{(2.24)}$$

$$\frac{\partial^2 U_2}{\partial \xi^2} = -C<\frac{\partial U_1}{\partial \xi}> - (\frac{\partial^2}{\partial s^2} + k^2)<U_0> + \xi\,(2C^2<\frac{\partial U_0}{\partial \xi}> - (\frac{\partial^2}{\partial s^2} + k^2)<\frac{\partial U_0}{\partial \xi}>) \quad \textbf{(2.25)}$$

$$[\frac{\partial U_2}{\partial \xi}] = -C<\frac{\partial U_1}{\partial \xi}> - (\frac{\partial^2}{\partial s^2} + k^2)<U_0> \quad \textbf{(2.26)}$$

$$\frac{\partial U_2}{\partial \xi} = <\frac{\partial U_2}{\partial \xi}> - C\xi<\frac{\partial U_1}{\partial \xi}> - \xi\,(\frac{\partial^2}{\partial s^2} + k^2)<U_0>$$

$$+\frac{1}{2}(\xi - \frac{1}{2})(\xi + \frac{1}{2})(2C^2<\frac{\partial U_0}{\partial \xi}> - (\frac{\partial^2}{\partial s^2} + k^2)<\frac{\partial U_0}{\partial \xi}>) \quad \textbf{(2.27)}$$

$$[U_2] = <\frac{\partial U_2}{\partial \xi}> - \frac{1}{12}(2C^2<\frac{\partial U_0}{\partial \xi}> - (\frac{\partial^2}{\partial s^2} + k^2)<\frac{\partial U_0}{\partial \xi}>) \quad \textbf{(2.28)}$$

$$U_2 = \langle U_2 \rangle + \xi \langle \frac{\partial U_2}{\partial \xi} \rangle - \frac{1}{2}(\xi - \frac{1}{2})(\xi + \frac{1}{2})\left(C\langle \frac{\partial U_1}{\partial \xi} \rangle + (\frac{\partial^2}{\partial s^2} + k^2)\langle U_0 \rangle\right)$$

$$+ \frac{1}{4}(\frac{2}{3}\xi^3 - \frac{1}{2}\xi)\left(2C^2 \langle \frac{\partial U_0}{\partial \xi} \rangle - (\frac{\partial^2}{\partial s^2} + k^2)\langle \frac{\partial U_0}{\partial \xi} \rangle\right) \quad \textbf{(2.29)}$$

The explicit form of derivation of 3^{rd} order thin layer conditions as follows:

$$\frac{\partial^2 U_3}{\partial \xi^2} = -\left(C\frac{\partial U_2}{\partial \xi} + 3\xi C \frac{\partial^2 U_2}{\partial \xi^2}\right)$$

$$-\left((\frac{\partial^2}{\partial s^2} + k^2) + 2\xi C^2 \frac{\partial}{\partial \xi} + 3(\xi C)^2 \frac{\partial^2}{\partial \xi^2}\right) U_1$$

$$-\left(\xi C(\frac{\partial^2}{\partial s^2} + 3k^2) - \xi C' \frac{\partial}{\partial s} + \xi^2 C^3 \frac{\partial}{\partial \xi} + (\xi C)^3 \frac{\partial^2}{\partial \xi^2}\right) U_0 \quad \textbf{(2.30)}$$

$$\frac{\partial^2 U_3}{\partial \xi^2} = -C\langle \frac{\partial U_2}{\partial \xi} \rangle + C^2 \xi \langle \frac{\partial U_1}{\partial \xi} \rangle + \xi C\,(\frac{\partial^2}{\partial s^2} + k^2)\langle U_0 \rangle$$

$$-\frac{C}{2}(\xi^2 - \frac{1}{4})\left(2C^2 \langle \frac{\partial U_0}{\partial \xi} \rangle - (\frac{\partial^2}{\partial s^2} + k^2)\langle \frac{\partial U_0}{\partial \xi} \rangle\right) + 3\xi C^2 \langle \frac{\partial U_1}{\partial \xi} \rangle$$

$$+ 3\xi C\,(\frac{\partial^2}{\partial s^2} + k^2)\langle U_0 \rangle - 3\xi^2 C\left(2C^2 \langle \frac{\partial U_0}{\partial \xi} \rangle - (\frac{\partial^2}{\partial s^2} + k^2)\langle \frac{\partial U_0}{\partial \xi} \rangle\right)$$

$$-(\frac{\partial^2}{\partial s^2} + k^2)\left(\langle U_1 \rangle - C\frac{1}{2}(\xi - \frac{1}{2})(\xi + \frac{1}{2})\langle \frac{\partial U_0}{\partial \xi} \rangle + \xi \langle \frac{\partial U_1}{\partial \xi} \rangle\right) - 2\xi C^2\left(\langle \frac{\partial U_1}{\partial \xi} \rangle - C\xi \langle \frac{\partial U_0}{\partial \xi} \rangle\right)$$

$$-3(\xi C)^2\left(-C\langle \frac{\partial U_0}{\partial \xi} \rangle\right) - \xi C\,(\frac{\partial^2}{\partial s^2} + 3k^2)\left(\langle U_0 \rangle + \xi \langle \frac{\partial U_0}{\partial \xi} \rangle\right)$$

$$+ \xi C' \frac{\partial}{\partial s}\left(\langle U_0 \rangle + \xi \langle \frac{\partial U_0}{\partial \xi} \rangle\right) - \xi^2 C^3 \langle \frac{\partial U_0}{\partial \xi} \rangle \quad \textbf{(2.31)}$$

$$[\frac{\partial U_3}{\partial \xi}] = -C\langle \frac{\partial U_2}{\partial \xi} \rangle + \frac{C}{12}\left(2C^2 \langle \frac{\partial U_0}{\partial \xi} \rangle - (\frac{\partial^2}{\partial s^2} + k^2)\langle \frac{\partial U_0}{\partial \xi} \rangle\right) - \frac{C^3}{12}\langle \frac{\partial U_0}{\partial \xi} \rangle$$

$$-\frac{3C}{12}\left(2C^2 \langle \frac{\partial U_0}{\partial \xi} \rangle - (\frac{\partial^2}{\partial s^2} + k^2)\langle \frac{\partial U_0}{\partial \xi} \rangle\right) - (\frac{\partial^2}{\partial s^2} + k^2)\left(\langle U_1 \rangle + \frac{C}{12}\langle \frac{\partial U_0}{\partial \xi} \rangle\right)$$

$$+\frac{1}{4}C^3 \langle \frac{\partial U_0}{\partial \xi} \rangle + \frac{1}{6}C^3 \langle \frac{\partial U_0}{\partial \xi} \rangle - \frac{1}{12}C(\frac{\partial^2}{\partial s^2} + 3k^2)\langle \frac{\partial U_0}{\partial \xi} \rangle + \frac{1}{12}C' \frac{\partial}{\partial s}\langle \frac{\partial U_0}{\partial \xi} \rangle \quad \textbf{(2.32)}$$

$$[\frac{\partial U_3}{\partial \xi}] = -C\langle \frac{\partial U_2}{\partial \xi} \rangle - (\frac{\partial^2}{\partial s^2} + k^2)\langle U_1 \rangle + \left(\frac{C^3}{6} - \frac{C}{12}\left(\frac{\partial^2}{\partial s^2} + k^2\right) + \frac{3C}{12}\left(\frac{\partial^2}{\partial s^2} + k^2\right)\right)\langle \frac{\partial U_0}{\partial \xi} \rangle$$

$$\left(-\frac{C^3}{2} - \frac{1}{12}(\frac{\partial^2}{\partial s^2} + k^2)\,C + \frac{C^3}{4} + \frac{C^3}{6} - \frac{C}{12}(\frac{\partial^2}{\partial s^2} + 3k^2) + \frac{1}{12}C' \frac{\partial}{\partial s} - \frac{C^3}{12}\right)\langle \frac{\partial U_0}{\partial \xi} \rangle \quad \textbf{(2.33)}$$

$$[\frac{\partial U_3}{\partial \xi}] = -C\langle \frac{\partial U_2}{\partial \xi} \rangle - (\frac{\partial^2}{\partial s^2} + k^2)\langle U_1 \rangle + (\frac{C}{12}\frac{\partial^2}{\partial s^2} - \frac{C}{6}k^2 + \frac{1}{12}C' \frac{\partial}{\partial s} - \frac{1}{12}\frac{\partial^2}{\partial s^2}C)\langle \frac{\partial U_0}{\partial \xi} \rangle \quad \textbf{(2.34)}$$

We can rearrange the terms so that

$$[\frac{\partial U_3}{\partial \xi}] = -C<\frac{\partial U_2}{\partial \xi}> - (\frac{\partial^2}{\partial s^2}+k^2)\,<U_1> + \frac{1}{12}(\frac{\partial}{\partial s}C\,\frac{\partial}{\partial s} - \frac{\partial^2}{\partial s^2}\,C - 2Ck^2 + C\,\frac{\partial^2}{\partial s^2})\,<\frac{\partial U_0}{\partial \xi}> \quad \textbf{(2.35)}$$

But in fact $<\frac{\partial U_0}{\partial \xi}> = 0$.

$$\frac{\partial^2 U_3}{\partial \xi^2} = -C<\frac{\partial U_2}{\partial \xi}> + C^2\xi\,<\frac{\partial U_1}{\partial \xi}> + \xi C\,(\frac{\partial^2}{\partial s^2}+k^2)\,<U_0> + 3\xi C^2<\frac{\partial U_1}{\partial \xi}>$$

$$+ 3\xi C\,(\frac{\partial^2}{\partial s^2}+k^2)\,<U_0> - (\frac{\partial^2}{\partial s^2}+k^2)\,(<U_1> + \xi<\frac{\partial U_1}{\partial \xi}>) - 2\xi C^2<\frac{\partial U_1}{\partial \xi}>$$

$$- \xi C\,(\frac{\partial^2}{\partial s^2}+3k^2)\,<U_0> + \xi C'\,\frac{\partial}{\partial s}<U_0> \quad \textbf{(2.36)}$$

$$\frac{\partial^2 U_3}{\partial \xi^2} = -C<\frac{\partial U_2}{\partial \xi}> - (\frac{\partial^2}{\partial s^2}+k^2)\,<U_1> + \xi\,(2C^2<\frac{\partial U_1}{\partial \xi}> - (\frac{\partial^2}{\partial s^2}+k^2)\,<\frac{\partial U_1}{\partial \xi}>)$$

$$+\xi\,(3C\,\frac{\partial^2}{\partial s^2} + Ck^2 + C'\,\frac{\partial}{\partial s})\,<U_0> \quad \textbf{(2.37)}$$

$$\frac{\partial U_3}{\partial \xi} = <\frac{\partial U_3}{\partial \xi}> - C\xi\,<\frac{\partial U_2}{\partial \xi}> - \xi(\frac{\partial^2}{\partial s^2}+k^2)<U_1> + \frac{1}{2}\,(\xi^2 - \frac{1}{4})\,(2C^2<\frac{\partial U_1}{\partial \xi}> - (\frac{\partial^2}{\partial s^2}+k^2)\,<\frac{\partial U_1}{\partial \xi}>)$$

$$+\frac{1}{2}\,(\xi^2 - \frac{1}{4})\,(3C\,\frac{\partial^2}{\partial s^2} + Ck^2 + C'\,\frac{\partial}{\partial s})\,<U_0> \quad \textbf{(2.38)}$$

$$[U_3] = <\frac{\partial U_3}{\partial \xi}> + \frac{1}{12}(\frac{\partial^2}{\partial s^2} + k^2 - 2C^2)\,<\frac{\partial U_1}{\partial \xi}> - \frac{1}{12}\,(3C\,\frac{\partial^2}{\partial s^2} + Ck^2 + C'\,\frac{\partial}{\partial s})\,<U_0> \quad \textbf{(2.39)}$$

$$U_3 = <U_3> + \xi<\frac{\partial U_3}{\partial \xi}> - C\,\frac{1}{2}\,(\xi^2 - \frac{1}{4})\,<\frac{\partial U_2}{\partial \xi}> - \frac{1}{2}\,(\xi^2 - \frac{1}{4})\,(\frac{\partial^2}{\partial s^2} + k^2)\,<U_1>$$

$$+\frac{1}{4}\,(\frac{2}{3}\xi^3 - \frac{1}{2}\xi)\,(2C^2<\frac{\partial U_1}{\partial \xi}> - (\frac{\partial^2}{\partial s^2}+k^2)\,<\frac{\partial U_1}{\partial \xi}>)$$

$$+\frac{1}{4}\,(\frac{2}{3}\xi^3 - \frac{1}{2}\xi)\,(3C\,\frac{\partial^2}{\partial s^2} + Ck^2 + C'\,\frac{\partial}{\partial s})\,<U_0> \quad \textbf{(2.40)}$$

The stages to derive 4^{th} order thin layer conditions as follows:

$$\frac{\partial^2 U_4}{\partial \xi^2} = -(C\,\frac{\partial U_3}{\partial \xi} + 3\xi C\,\frac{\partial^2 U_3}{\partial \xi^2}) - ((\frac{\partial^2}{\partial s^2}+k^2) + 2\xi C^2\,\frac{\partial}{\partial \xi} + 3(\xi C)^2\,\frac{\partial^2}{\partial \xi^2})\,U_2$$

$$-(\xi C(\frac{\partial^2}{\partial s^2}+3k^2) - \xi C'\,\frac{\partial}{\partial s} + \xi^2 C^3\,\frac{\partial}{\partial \xi} + (\xi C)^3\,\frac{\partial^2}{\partial \xi^2})U_1 - 3(\xi C)^2 k^2 U_0 \quad \textbf{(2.41)}$$

$$\frac{\partial^2 U_4}{\partial \xi^2} = -C<\frac{\partial U_3}{\partial \xi}> + C^2\xi<\frac{\partial U_2}{\partial \xi}> + C\xi\,(\frac{\partial^2}{\partial s^2}+k^2)\,<U_1> + 3\xi C^2<\frac{\partial U_2}{\partial \xi}>$$

$$- C\,\frac{1}{2}\,(\xi^2 - \frac{1}{4})\,(2C^2<\frac{\partial U_1}{\partial \xi}> - (\frac{\partial^2}{\partial s^2}+k^2)\,<\frac{\partial U_1}{\partial \xi}>) + 3\xi C\,(\frac{\partial^2}{\partial s^2}+k^2)\,<U_1>$$

$$-C\,\frac{1}{2}\,(\xi^2 - \frac{1}{4})\,(3C\,\frac{\partial^2}{\partial s^2} + Ck^2 + C'\,\frac{\partial}{\partial s})\,<U_0> - 3(\xi C)^2 k^2 < U_0 >$$

$$-3\xi^2 C\,(2C^2<\frac{\partial U_1}{\partial \xi}> - (\frac{\partial^2}{\partial s^2}+k^2)\,<\frac{\partial U_1}{\partial \xi}>) - 3\xi^2 C\,(3C\,\frac{\partial^2}{\partial s^2} + Ck^2 + C'\,\frac{\partial}{\partial s})\,<U_0>$$

$$-\left(\xi \mathrm{C}\left(\frac{\partial^2}{\partial s^2}+3k^2\right)-\xi C'\frac{\partial}{\partial s}+\xi^2 C^3\frac{\partial}{\partial \xi}+(\xi C)^3\frac{\partial^2}{\partial \xi^2}\right)\left(<U_1>+\xi<\frac{\partial U_1}{\partial \xi}>\right)$$

$$+\left(\left(\frac{\partial^2}{\partial s^2}+k^2\right)+2\xi C^2\frac{\partial}{\partial \xi}+3(\xi \mathrm{C})^2\frac{\partial^2}{\partial \xi^2}\right)\frac{1}{2}(\xi^2-\frac{1}{4})(C<\frac{\partial U_1}{\partial \xi}>+(\frac{\partial^2}{\partial s^2}+k^2)<U_0>)$$

$$-\left(\left(\frac{\partial^2}{\partial s^2}+k^2\right)+2\xi C^2\frac{\partial}{\partial \xi}+3(\xi \mathrm{C})^2\frac{\partial^2}{\partial \xi^2}\right)\left(<U_2>+\xi<\frac{\partial U_2}{\partial \xi}>\right) \quad \textbf{(2.42)}$$

$$[\frac{\partial U_4}{\partial \xi}]=-\mathrm{C}<\frac{\partial U_3}{\partial \xi}>+\frac{C}{12}(2C^2<\frac{\partial U_1}{\partial \xi}>-(\frac{\partial^2}{\partial s^2}+k^2)<\frac{\partial U_1}{\partial \xi}>)+\frac{C}{12}(3C\frac{\partial^2}{\partial s^2}+Ck^2+C'\frac{\partial}{\partial s})<U_0>$$

$$-\frac{C}{4}(2C^2<\frac{\partial U_1}{\partial \xi}>-(\frac{\partial^2}{\partial s^2}+k^2)<\frac{\partial U_1}{\partial \xi}>)-\frac{C}{4}(3C\frac{\partial^2}{\partial s^2}+Ck^2+C'\frac{\partial}{\partial s})<U_0>$$

$$-(\frac{\partial^2}{\partial s^2}+k^2)<U_2>-\frac{C^2}{4}\frac{\partial^2}{\partial \xi^2}<U_2>-\frac{C^2}{6}\frac{\partial}{\partial \xi}<\frac{\partial U_2}{\partial \xi}>-\frac{1}{12}(\frac{\partial^2}{\partial s^2}+k^2)\,C<\frac{\partial U_1}{\partial \xi}>$$

$$-\frac{1}{12}(\frac{\partial^2}{\partial s^2}+k^2)(\frac{\partial^2}{\partial s^2}+k^2)<U_0>-\frac{1}{80}C^2\frac{\partial^2}{\partial \xi^2}C<\frac{\partial U_1}{\partial \xi}>-\frac{1}{80}C^2\frac{\partial^2}{\partial \xi^2}(\frac{\partial^2}{\partial s^2}+k^2)<U_0>$$

$$-\frac{1}{12}C^3\frac{\partial}{\partial \xi}<U_1>-\frac{1}{12}C(\frac{\partial^2}{\partial s^2}+3k^2)<\frac{\partial U_1}{\partial \xi}>+\frac{1}{12}C'\frac{\partial}{\partial s}<\frac{\partial U_1}{\partial \xi}>-\frac{1}{80}C^3\frac{\partial^2}{\partial \xi^2}<\frac{\partial U_1}{\partial \xi}>$$

$$-\frac{1}{4}C^2k^2<U_0> \quad \textbf{(2.43)}$$

$$\frac{\partial U_4}{\partial \xi}=<\frac{\partial U_4}{\partial \xi}>-\mathrm{C}\xi<\frac{\partial U_3}{\partial \xi}>+\frac{1}{2}(\xi^2-\frac{1}{4})C^2<\frac{\partial U_2}{\partial \xi}>+\frac{1}{2}(\xi^2-\frac{1}{4})C(\frac{\partial^2}{\partial s^2}+k^2)<U_1>$$

$$+3\frac{1}{2}(\xi^2-\frac{1}{4})C^2<\frac{\partial U_2}{\partial \xi}>-C\frac{1}{4}(\frac{2}{3}\xi^3-\frac{1}{2}\xi)(2C^2<\frac{\partial U_1}{\partial \xi}>-(\frac{\partial^2}{\partial s^2}+k^2)<\frac{\partial U_1}{\partial \xi}>)$$

$$+\frac{1}{2}(\xi^2-\frac{1}{4})3C(\frac{\partial^2}{\partial s^2}+k^2)<U_1>-C\frac{1}{4}(\frac{2}{3}\xi^3-\frac{1}{2}\xi)(3C\frac{\partial^2}{\partial s^2}+Ck^2+C'\frac{\partial}{\partial s})<U_0>$$

$$-\xi^3C(2C^2<\frac{\partial U_1}{\partial \xi}>-(\frac{\partial^2}{\partial s^2}+k^2)<\frac{\partial U_1}{\partial \xi}>)-\xi^3C(3C\frac{\partial^2}{\partial s^2}+Ck^2+C'\frac{\partial}{\partial s})<U_0>$$

$$-\mathrm{C}\frac{1}{2}(\xi^2-\frac{1}{4})\left(\frac{\partial^2}{\partial s^2}+3k^2\right)<U_1>+\frac{1}{2}(\xi^2-\frac{1}{4})C'\frac{\partial}{\partial s}<U_1>$$

$$-\frac{1}{3}\xi^3C^3\frac{\partial}{\partial \xi}<U_1>-\frac{1}{2}(\frac{\xi^4}{2}-\frac{1}{32})(C)^3\frac{\partial^2}{\partial \xi^2}<U_1>+\frac{1}{3}\xi^3C'\frac{\partial}{\partial s}<\frac{\partial U_1}{\partial \xi}>$$

$$-\frac{1}{3}\xi^3\mathrm{C}\left(\frac{\partial^2}{\partial s^2}+3k^2\right)<\frac{\partial U_1}{\partial \xi}>-\frac{1}{2}\left(\frac{\xi^4}{2}-\frac{1}{32}\right)C^3\frac{\partial}{\partial \xi}<\frac{\partial U_1}{\partial \xi}>$$

$$-\frac{\xi^5}{5}(C)^3\frac{\partial^2}{\partial \xi^2}<\frac{\partial U_1}{\partial \xi}>-(\frac{\partial^2}{\partial s^2}+k^2)\xi<U_2>-2\frac{1}{2}(\xi^2-\frac{1}{4})C^2\frac{\partial}{\partial \xi}<U_2>$$

$$-\xi^3(\mathrm{C})^2\frac{\partial^2}{\partial \xi^2}<U_2>-\frac{1}{2}(\xi^2-\frac{1}{4})(\frac{\partial^2}{\partial s^2}+k^2)<\frac{\partial U_2}{\partial \xi}>-2\frac{1}{3}\xi^3C^2\frac{\partial}{\partial \xi}<\frac{\partial U_2}{\partial \xi}>$$

$$-3\frac{1}{2}(\frac{\xi^4}{2}-\frac{1}{32})C^2\frac{\partial^2}{\partial \xi^2}<\frac{\partial U_2}{\partial \xi}>-\xi^3C^2k^2<U_0>+\frac{1}{4}(\frac{2}{3}\xi^3-\frac{1}{2}\xi)(\frac{\partial^2}{\partial s^2}+k^2)\,\mathrm{C}<\frac{\partial U_1}{\partial \xi}>$$

$$+\frac{1}{4}\left(\frac{2}{3}\xi^3-\frac{1}{2}\xi\right)\left(\frac{\partial^2}{\partial s^2}+k^2\right)\left(\frac{\partial^2}{\partial s^2}+k^2\right)<U_0>+\frac{1}{2}C^2\frac{\partial}{\partial\xi}\left(\frac{\xi^4}{2}-\frac{\xi^2}{4}+\frac{1}{32}\right)C<\frac{\partial U_1}{\partial\xi}>$$

$$+\frac{1}{2}C^2\frac{\partial}{\partial\xi}\left(\frac{\xi^4}{2}-\frac{\xi^2}{4}+\frac{1}{32}\right)\left(\frac{\partial^2}{\partial s^2}+k^2\right)<U_0>+3\frac{1}{4}\left(\frac{2\xi^5}{5}-\frac{\xi^3}{6}\right)C^2\frac{\partial^2}{\partial\xi^2}C<\frac{\partial U_1}{\partial\xi}>$$

$$+3\frac{1}{4}\left(\frac{2\xi^5}{5}-\frac{\xi^3}{6}\right)C^2\frac{\partial^2}{\partial\xi^2}\left(\frac{\partial^2}{\partial s^2}+k^2\right)<U_0> \quad \textbf{(2.44)}$$

$$[U_4]=<\frac{\partial U_4}{\partial\xi}>-\frac{1}{12}\left(C^2<\frac{\partial U_2}{\partial\xi}>+C\left(\frac{\partial^2}{\partial s^2}+k^2\right)<U_1>+3C^2<\frac{\partial U_2}{\partial\xi}>\right)-\frac{C}{4}\left(\frac{\partial^2}{\partial s^2}+k^2\right)<U_1>$$

$$+C\frac{1}{12}\left(\frac{\partial^2}{\partial s^2}+3k^2\right)<U_1>-\frac{1}{12}C'\frac{\partial}{\partial s}<U_1>+\frac{1}{80}C^3\frac{\partial^2}{\partial\xi^2}<U_1>$$

$$+\frac{1}{80}C^3\frac{\partial}{\partial\xi}<\frac{\partial U_1}{\partial\xi}>+\frac{1}{6}C^2\frac{\partial}{\partial\xi}<U_2>+\frac{1}{12}\left(\frac{\partial^2}{\partial s^2}+k^2\right)<\frac{\partial U_2}{\partial\xi}>$$

$$+\frac{3}{80}C^2\frac{\partial^2}{\partial\xi^2}<\frac{\partial U_2}{\partial\xi}>+\frac{1}{120}C^2\frac{\partial}{\partial\xi}C<\frac{\partial U_1}{\partial\xi}>+\frac{1}{120}C^2\frac{\partial}{\partial\xi}\left(\frac{\partial^2}{\partial s^2}+k^2\right)<U_0> \quad \textbf{(2.45)}$$

After all evaluations, using boundary conditions (2.2), we obtain 2nd order thin layer conditions as follows:

$$[U]=\delta<\frac{\partial U}{\partial n}>+0\left(\delta^2\right) \quad \textbf{(2.46)}$$

$$\left[\frac{\partial U}{\partial n}\right]=-C\,\delta<\frac{\partial U}{\partial n}>-\delta\left(\frac{\partial^2}{\partial s^2}+k^2\right)<U>+0\left(\delta^2\right) \quad \textbf{(2.47)}$$

We can write 3^{rd} order thin layer conditions in implicit form as follows:

$$[U]=\delta<\frac{\partial U}{\partial n}>+\frac{\delta^3}{12}\left(\frac{\partial^2}{\partial s^2}+k^2-2C^2\right)<\frac{\partial U}{\partial n}>$$

$$-\frac{\delta^3}{12}\left(3C\frac{\partial^2}{\partial s^2}+Ck^2+C'\frac{\partial}{\partial s}\right)<U>+0\left(\delta^3\right) \quad \textbf{(2.48)}$$

$$\left[\frac{\partial U}{\partial n}\right]=-C\,\delta<\frac{\partial U}{\partial n}>-\delta\left(\frac{\partial^2}{\partial s^2}+k^2\right)<U>+0\left(\delta^3\right) \quad \textbf{(2.49)}$$

Finally, we revise (2.43) and (2.45) to form 4^{th} order TLC as follows:

$$[U]=\delta<\frac{\partial U}{\partial n}>+\frac{\delta^3}{12}\left(\frac{\partial^2}{\partial s^2}+k^2-2C^2\right)<\frac{\partial U}{\partial n}>$$

$$-\frac{\delta^3}{12}\left(3C\frac{\partial^2}{\partial s^2}+Ck^2+C'\frac{\partial}{\partial s}\right)<U>+0\left(\delta^4\right) \quad \textbf{(2.50)}$$

$$\left[\frac{\partial U}{\partial n}\right]=-C\,\delta<\frac{\partial U}{\partial n}>-\delta\left(\frac{\partial^2}{\partial s^2}+k^2\right)<U>$$

$$-\frac{\delta^3}{12}\left(\frac{\partial^2}{\partial s^2}C+2Ck^2-C\frac{\partial^2}{\partial s^2}-C'\frac{\partial}{\partial s}\right)<\frac{\partial U}{\partial n}>$$

$$-\frac{\delta^3}{12}\left(\left(\frac{\partial^2}{\partial s^2}+k^2\right)\left(\frac{\partial^2}{\partial s^2}+k^2\right)+C^2\frac{\partial^2}{\partial s^2}+2CC'\frac{\partial}{\partial s}\right)<U>+0\left(\delta^4\right) \quad \textbf{(2.51)}$$

2.2 Solution of Generalized Thin Layer Conditions

In this section, solution method of 2nd and 4th order thin layer conditions are given by means of variational sense.

The solution procedure of 2nd order thin layer conditions with variational method as follows:

$$[U] = \delta \left\langle \frac{\partial U}{\partial n} \right\rangle \tag{2.52}$$

$$\left[\frac{\partial U}{\partial n}\right] = -\,C\,\delta \left\langle \frac{\partial U}{\partial n} \right\rangle - \delta \left(\frac{\partial^2}{\partial s^2} + k^2\right) \langle U \rangle \tag{2.53}$$

where $[U] = U^+ - U^-$ and $\left[\frac{\partial U}{\partial n}\right] = \frac{\partial U^+}{\partial n} - \frac{\partial U^-}{\partial n}$. U^+ and $\frac{\partial U^+}{\partial n}$ symbolize the field and the normal derivative of the field at the upper boundary of the thin layer, respectively and U^- and $\frac{\partial U^-}{\partial n}$ symbolize the field and the normal derivative of the field at the lower boundary of the thin layer, respectively. Here we introduce new auxiliary functions as follow,

$$\phi = \langle U \rangle = \frac{U^+ + U^-}{2} \tag{2.54}$$

$$\Psi = \left\langle \frac{\partial U}{\partial n} \right\rangle = \frac{1}{2}\left(\frac{\partial U^+}{\partial n} + \frac{\partial U^-}{\partial n}\right) \tag{2.55}$$

Using (2.54) and (2.55), 2nd order thin layer conditions can be rewritten as

$$2U^+ - 2\phi = \delta\,\Psi \tag{2.56}$$

$$2\,\frac{\partial U^+}{\partial n} - 2\Psi = -\,C\,\delta\,\Psi - \delta\left(\frac{\partial^2}{\partial s^2} + k^2\right)\phi \tag{2.57}$$

To solve equations (2.56) and (2.57) in variational sense, auxiliary functions ϕ and Ψ are written sum of basis functions with unknown coefficients c and d.

$$\phi = \sum c_j \phi_j(x) \tag{2.58}$$

$$\Psi = \sum d_j \Psi_j(x) \tag{2.59}$$

Here we use the roof top basis function for both Φ and Ψ, as follows:

$$\Phi_i(x) = \Psi_i(x) = \begin{cases} \frac{x - x_{i-1}}{x_i - x_{i-1}}, & x_{i-1} < x < x_i \\ \frac{x_{i+1} - x}{x_{i+1} - x_i}, & x_i < x < x_{i+1} \end{cases} \tag{2.60}$$

Then, we multiply both sides of equations (2.56) and (2.57) with same roof top test function, and integrate it, we obtain followings

$$\int 2U^{+}\Phi_i = 2\sum c_j \int \Phi_j\Phi_i + \delta \sum d_j \int \Psi_j\Phi_i \quad \textbf{(2.61)}$$

$$2\int \frac{\partial U^{+}}{\partial n}\Phi_i = 2\sum d_j \int \Psi_j\Phi_i - \delta \sum d_j \int C\,\Psi_j\Phi_i + \delta\sum c_j \int \frac{\partial}{\partial s}\Phi_j \frac{\partial}{\partial s}\Phi_i - \delta k^2 \sum c_j \int \Phi_j\Phi_i \quad \textbf{(2.62)}$$

After all these steps, we can write (2.61) and (2.62), in matrix form as

$$\begin{bmatrix} 2M_1 & \delta M_1 \\ \delta M_3 - \delta k^2 M_1 & 2M_1 - \delta M_2 \end{bmatrix} \begin{bmatrix} C \\ D \end{bmatrix} = \begin{bmatrix} f_1 \\ f_2 \end{bmatrix} \quad \textbf{(2.63)}$$

where M_1, M_2 and M_3 are defined as $\int \Phi_j\Phi_i$ and/or $\int \Psi_j\Phi_i$, $\int C\,\Psi_j\Phi_i$, $\int \frac{\partial}{\partial s}\Phi_j \frac{\partial}{\partial s}\Phi_i$, respectively and right-hand side of the equation system, f_1 and f_2 are defined as $\int 2U^{+}\Phi_i$, $\int 2\frac{\partial U^{+}}{\partial n}\Phi_i$, respectively. C is the vector of unknown coefficient c and D is the vector of unknown coefficient d. We solve (2.63) to obtain unknown coefficients c and d and then using c and d, U^{-} and $\frac{\partial U^{-}}{\partial n}$ are obtained.

The solution procedure of 4th order thin layer conditions is much more complex than the 2nd order's. In this section, we just give outline of the solution of 4th order thin layer conditions.

$$[\mathrm{U}] = \delta \left\langle \frac{\partial U}{\partial n} \right\rangle + \frac{\delta^3}{12}\left(\frac{\partial^2}{\partial s^2} + k^2 - 2C^2\right) \left\langle \frac{\partial U}{\partial n} \right\rangle - \frac{\delta^3}{12}\left(3C\,\frac{\partial^2}{\partial s^2} + Ck^2 + C'\frac{\partial}{\partial s}\right) \langle \mathrm{U} \rangle \quad \textbf{(2.64)}$$

$$\left[\frac{\partial U}{\partial n}\right] = -\,C\,\delta \left\langle \frac{\partial U}{\partial n} \right\rangle - \delta\left(\frac{\partial^2}{\partial s^2} + k^2\right) \langle \mathrm{U} \rangle - \frac{\delta^3}{12}\left(\frac{\partial^2}{\partial s^2} C + 2Ck^2 - C\frac{\partial^2}{\partial s^2} - C'\frac{\partial}{\partial s}\right) \left\langle \frac{\partial U}{\partial n} \right\rangle - \frac{\delta^3}{12}\left(\left(\frac{\partial^2}{\partial s^2} + k^2\right)\left(\frac{\partial^2}{\partial s^2} + k^2\right) + C^2\frac{\partial^2}{\partial s^2} + 2\,C\,C'\frac{\partial}{\partial s}\right) \langle \mathrm{U} \rangle \quad \textbf{(2.65)}$$

Here we introduce again auxiliary functions as follows:

$$\Psi_1 = \left(1 + \frac{\delta^2}{12}\left(\frac{\partial^2}{\partial s^2} + k^2\right)\right)\Psi \quad \textbf{(2.66)}$$

$$\Phi_1 = \left(1 + \frac{\delta^2}{12}\left(\frac{\partial^2}{\partial s^2} + k^2\right)\right)\Phi \quad \textbf{(2.67)}$$

Using (2.66), (2.67), (2.64) and (2.65) can be rewritten as

$$2U^{+} - 2\Phi = \delta\,\Psi_1 - \frac{\delta^3 C^2}{6}\Psi - \frac{\delta^3}{12}\left(3C\,\frac{\partial^2}{\partial s^2} + Ck^2 + C'\frac{\partial}{\partial s}\right)\Phi \quad \textbf{(2.68)}$$

$$2\frac{\partial U^{+}}{\partial n} - 2\Psi = -\delta\left(\frac{\partial^2}{\partial s^2} + k^2\right)\Phi_1 - C\,\delta\,\Psi - \frac{\delta^3}{12}\left(\frac{\partial}{\partial s}C' + 2Ck^2\right)\Psi$$

$$- \frac{\delta^3}{12}\left(\frac{\partial}{\partial s}C^2\frac{\partial}{\partial s}\right)\Phi \qquad \textbf{(2.69)}$$

If we use the Taylor expansion, the equations (2.68) and (2.69) can be rewritten as

$$\Psi_1 - \frac{\delta^2}{12}\left(\frac{\partial^2}{\partial s^2} + k^2\right)\Psi_1 = \Psi \qquad \textbf{(2.70)}$$

$$\Phi_1 - \frac{\delta^2}{12}\left(\frac{\partial^2}{\partial s^2} + k^2\right)\Phi_1 = \Phi \qquad \textbf{(2.71)}$$

After that, same procedure which is explained for 2nd order is applied for solution and we obtain the following linear equation system

$$\begin{bmatrix} H_{11} & H_{12} & H_{13} & H_{14} \\ H_{21} & H_{22} & H_{23} & H_{24} \\ H_{31} & H_{32} & H_{33} & H_{34} \\ H_{41} & H_{42} & H_{43} & H_{44} \end{bmatrix}\begin{bmatrix} C \\ D \\ C_1 \\ D_1 \end{bmatrix} = \begin{bmatrix} f_1 \\ f_2 \\ 0 \\ 0 \end{bmatrix} \qquad \textbf{(2.72)}$$

where c, d, c_1 and d_1 are unknown coefficients. After solve this equation, U^{-} and $\frac{\partial U^{-}}{\partial n}$ are obtained.

The details of computations of 4th order thin layer approximation are given at Appendix. Notice that computation cost of realization of 4th order thin layer approximation is more than 2nd order thin layer approximation.

3. RECIPROCITY GAP LINEAR SAMPLING METHOD

The inverse problem we are interested in is that of determining the location and shape of buried objects under a layered medium. The geometry of the problem is shown in Figure 3.1. The scatterers D_1, D_2 buried in the lower medium can be made of perfect conductors, dielectrics or combinations of two. The total electric field due to point source located at x_0 is given by $E = (0,0,u(.;x_0))$ and satisfies the Helmholtz equation,

$$\Delta u(.;x_0) + k_0^2 n\, u(.;x_0) = -\delta_{x_0} \qquad in\ \mathbb{R}^2 \backslash D \tag{3.1}$$

where k_0 denotes the wavenumber in the air and where n denotes the medium index: $n(x) = 1$ in the air and $n(x) = n$ (constant) in the lower medium. We shall set $k_1 = k_0\sqrt{n}$ where the square root is the one with non negative imaginary part.

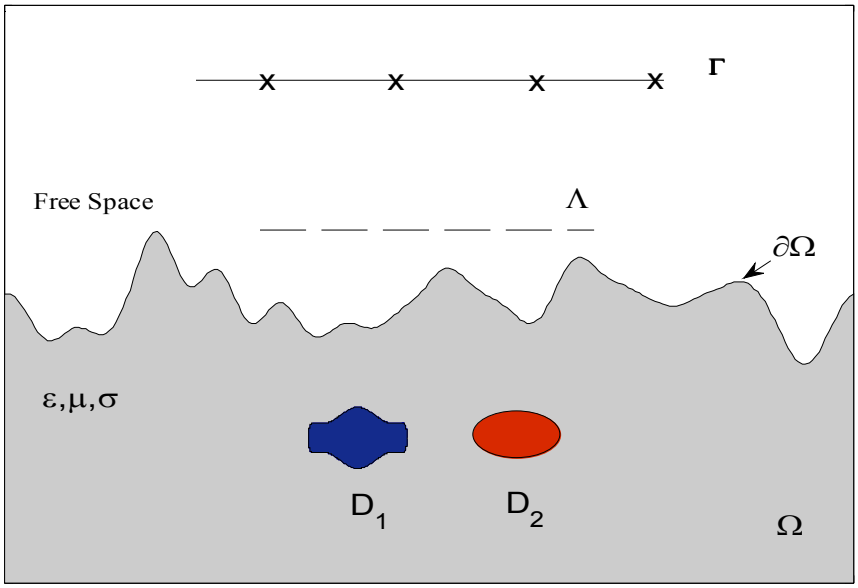

Figure 3.1 : Explicative Example

In the sequel, we explain the principle of the RG-LSM method assuming field data $u(x,x_0)$ and its normal derivative $\partial u(x,x_0)/\partial n$ are known for all $x \in \partial\Omega$ and

$x_0 \in \Gamma$ (see Figure 3.1). Note that these data can be obtained by direct measurement in the case of two layered medium, and for multi-layered medium, data needed on the lowest interface can be deduced from measurement data by using TLC. Let v be a field satisfying the Helmholtz equation in Ω. We define the *Reciprocity Gap* between $u(x, x_0)$ and v by

$$\mathcal{R}(u(x,x_0),v) := \int_{\partial\Omega} \left(u(x,x_0)\frac{\partial \upsilon}{\partial \mathrm{n}}(x) - \upsilon(x)\frac{\partial u(x,x_0)}{\partial \mathrm{n}} \right) ds(x) \qquad \textbf{(3.2)}$$

In this work, we have chosen υ as a *single layer potential* defined by

$$\upsilon = s_g = \int_\Lambda g(y)\Phi(x,y)ds(y) \qquad \textbf{(3.3)}$$

where g is an unknown potential and $\Phi(x,y) = \frac{i}{4}H_0^{(1)}(k_1|x-y|)$ with $H_0^{(1)}$ being the Hankel function of the first kind with order zero and Λ being a straight horizontal line in the upper medium (see Figure 3.1). Let us note that, in principle, one can use any other surface integral operator instead of the single layer potential, as long as it provides a (dense) subset of the solutions to the Helmholtz equation in $\Omega \backslash D$.

The RG-LSM solve the following integral equation to find an approximation solution $g_z \in L^2(\Lambda)$ to the integral equation

$$\mathcal{R}\big(u(.;x_0), s_{g_z}\big) \cong \mathcal{R}\big(u(.;x_0), \Phi(.,z)\big) \qquad x_0 \in \Gamma \qquad \textbf{(3.4)}$$

where z is a parameter, so-called sampling point, lying in the search domain in Ω. In other words, for a given sampling point $z \in D$, we would like to test whether there exists a regular solution to the Helmholtz equation in Ω, namely, s_{g_z}, whose reciprocity gap with $u(.;x_0)$ coincides with reciprocity gap of singular solution, namely $\Phi(.,z)$, with the same fields and for all sources x_0.

One can easily guess that this would not be true when z is outside D since $u(.;x_0)$ and s_{g_z} satisfy the equation with -δ_z source term. The method then stipulates that given an approximate solution to (3.4), the norm of $\|g_z\|$ would be much larger for z outside D than for z inside D.

To compute an approximate solution to the ill-posed equation (3.4), one can use Tikhonov regularization combined with the Morozov discrepancy principle for the choice of regularization parameter.

The numerical procedure to locate object is then the following: uniform sampling points $\{z_i\}_{i=1,\dots,N}$ of the search domain are the considered and for each point z_i

$$\mathcal{G}(z_i) = \|\phi(.,z_i)\|_{L^2(\Gamma)} / \|g_{z_{i,\alpha}}\|_{L^2(\Lambda)} \quad \textbf{(3.5)}$$

is computed where $\phi(x_0,z) = \mathcal{R}\big(u(.;x_0),\Phi(.,z)\big)$ $x_0 \in \Gamma$, $z \in \Omega$. Then the contours of the function $z_i \to \mathcal{G}(z_i)$ are plotted. As explained above, the values of $\mathcal{G}$ are expected to be much smaller where z_i does not belong the scatterers. Let us notice that, in theory there is no link between the choice of Λ and Γ. However, in order to end up square linear system, we choose equal number of discretization points on both of them but with different step size : $\sim \frac{2\pi}{10k_0}$ for Γ and $\sim \frac{2\pi}{10k_1}$ for Λ.

4. NUMERICAL RESULTS

In this section, numerical results that are obtained via using thin layer conditions and Reciprocity Gap Linear Sampling Method. The main purpose is to analyze the thin layer conditions' approximation to the exact values and to examine thin layer conditions' effects to RG-LSM results.

Numerical results are presented for three different interfaced thin layers: flat interface, rough interface and finally circular interface for cylindrical medium.

For all examples, the frequency of exciting sources is chosen as $f = 300\ MHz$ which corresponds $\lambda_0 = 1$, where λ_0 is the wavelength of the free space. And also for all examples, the number of sources is chosen as 60 and they are placed in free space. Measurement fields are obtained synthetically by solving forward scattering problem using an integral equation method.

4.1. Numerical Results For Flat Interfaces

Firstly, reconstruction of objects buried in a layered medium is done for flat interfaces. Geometry and parameters of examples are shown in Figure 4.1.

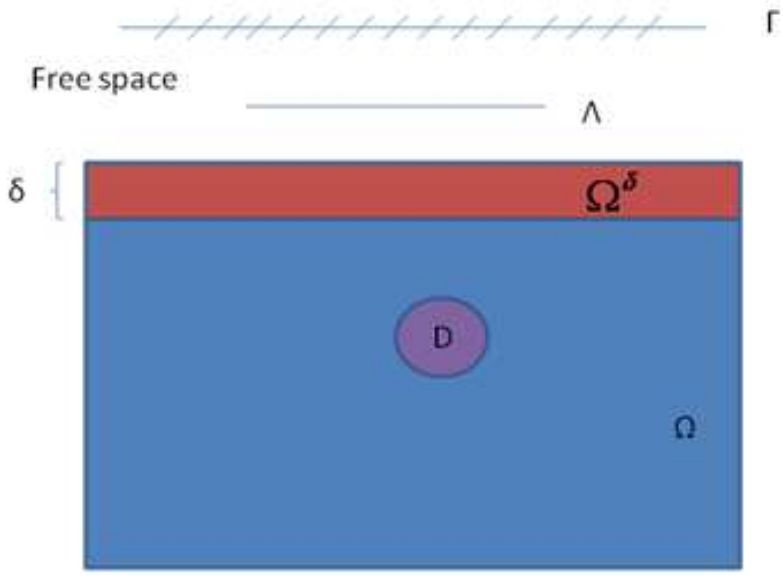

Figure 4.1 : General structure of the problem in flat case

Here $\Gamma, D, \Omega, \Omega^{\delta}, \delta$ and Λ symbolize sources, object buried, lower homogeneous medium, thin layer, thickness of thin layer and single layer potential which is used in Reciprocity Gap Linear Sampling Method, respectively.

Example 4.1.1. In the first example, thin layer is placed between free space and homogeneous media with $\varepsilon_r = 1.5 + 0.2i$. Thickness of the thin layer is chosen as $\delta = 0.1\lambda_0$ and relative permittivity of the thin layer is chosen as $\varepsilon_{r_\delta} = 2.5 + 0.2i$. Perfectly conducting rectangle-shaped object with dimensions $\lambda_0 \times \lambda_0/2$ is buried in a lower homogeneous medium. All exciting sources are located in only upper part.

For this thickness, the field and its normal derivative at the lower boundary of the thin layer are approximated with 2nd and 4th order thin layer conditions. Comparison of approximated and exact field and normal derivative of the field are given Figure 4.2 and Figure 4.3, respectively. It can be seen from Figure 4.2 and Figure 4.3, 2nd order condition is enough for approximation of fields, because of the small thickness of the layer.

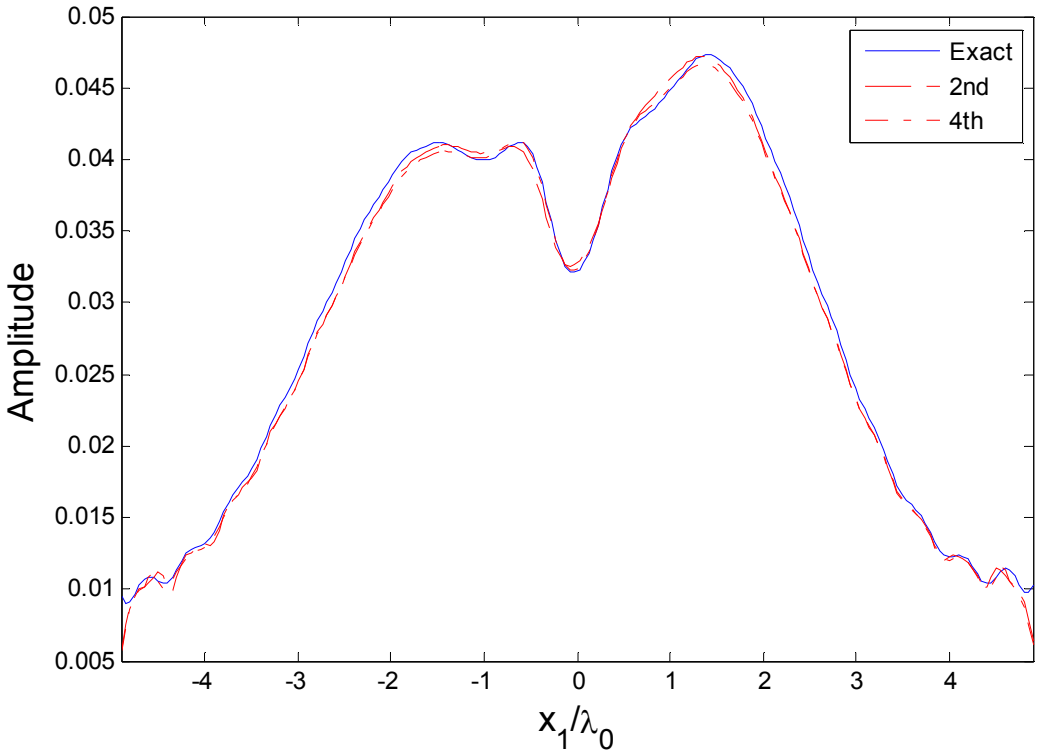

Figure 4.2 : Comparison of the fields at the lower boundary of the thin layer for Example 4.1.1

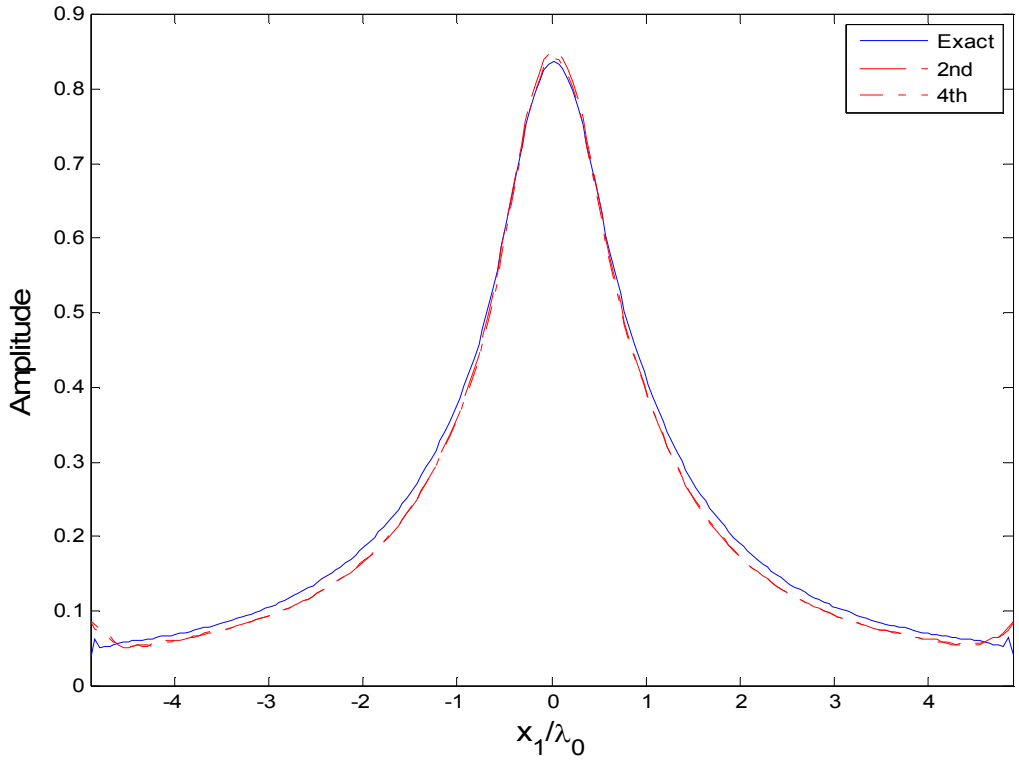

Figure 4.3 : Comparison of normal derivatives of the fields at the lower boundary of the thin layer for Example 4.1.1

Then, reconstructions of the object with exact data and data obtained by 2^{nd} and 4^{th} order TLC are done and presented in Figure 4.4, Figure 4.5 and Figure 4.6, respectively. The dashed lines symbolize the exact boundary of the object. From these figures, it is obvious that the object can be successfully reconstructed by using approximated data.

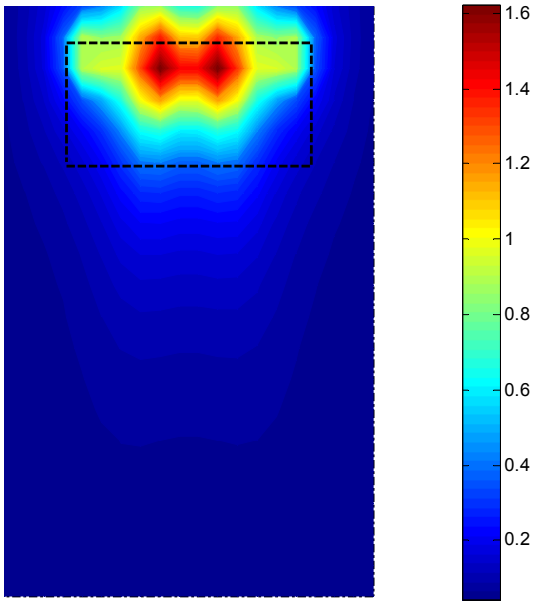

Figure 4.4 : Reconstruction associated with exact data for Example 4.1.1

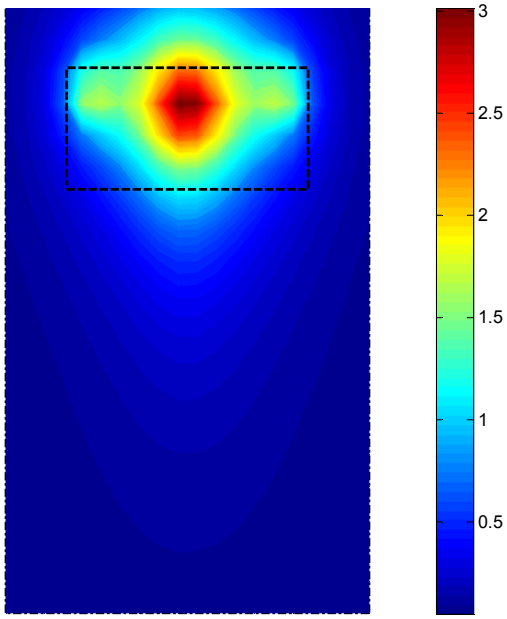

Figure 4.5 : Reconstruction associated with 2nd order TLC for Example 4.1.1

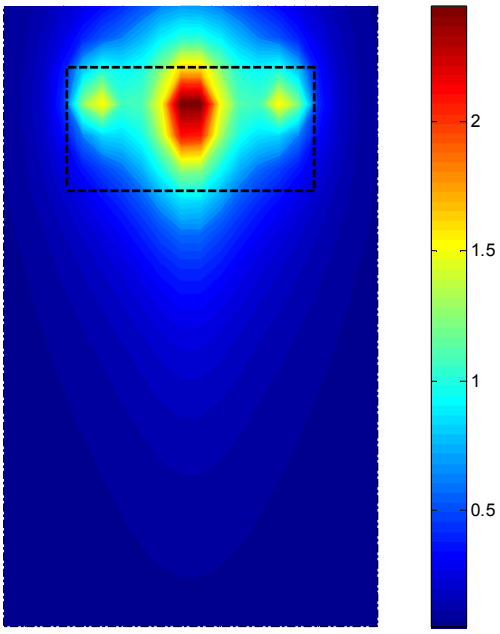

Figure 4.6 : Reconstruction associated with 4th order TLC for Example 4.1.1

Example 4.1.2. In the second example, δ is increased from $0.1\lambda_0$ to $0.3\lambda_0$ to examine the effect of the thickness. Everything else stays the same as in Example 4.1.1. Figure 4.7 and Figure 4.9 show the comparison of field and its normal derivative. As it is expected, when the thickness is larger, 4th order TLC gives much better approximation than 2nd order TLC. However, even 4th order TLC does not approximate the exact field as well as the Example 4.1.1 . The reason for this is that accuracy of the TLC depends on thickness, δ, see Equations(2.46-2.51), smaller thickness gives better approximation. Therefore to improve our result, we assume that this large thickness, $\delta = 0.3\lambda_0$ can be thought of combination of two same layer with thickness, $\delta_{1,2} = 0.15\lambda_0$ and we applied thin layer conditions two times which we called it as cascaded thin layer condition. With cascaded 4th order TLC, almost exact field values are obtained, even though thickness is large, see Figure 4.8 and Figure 4.10.

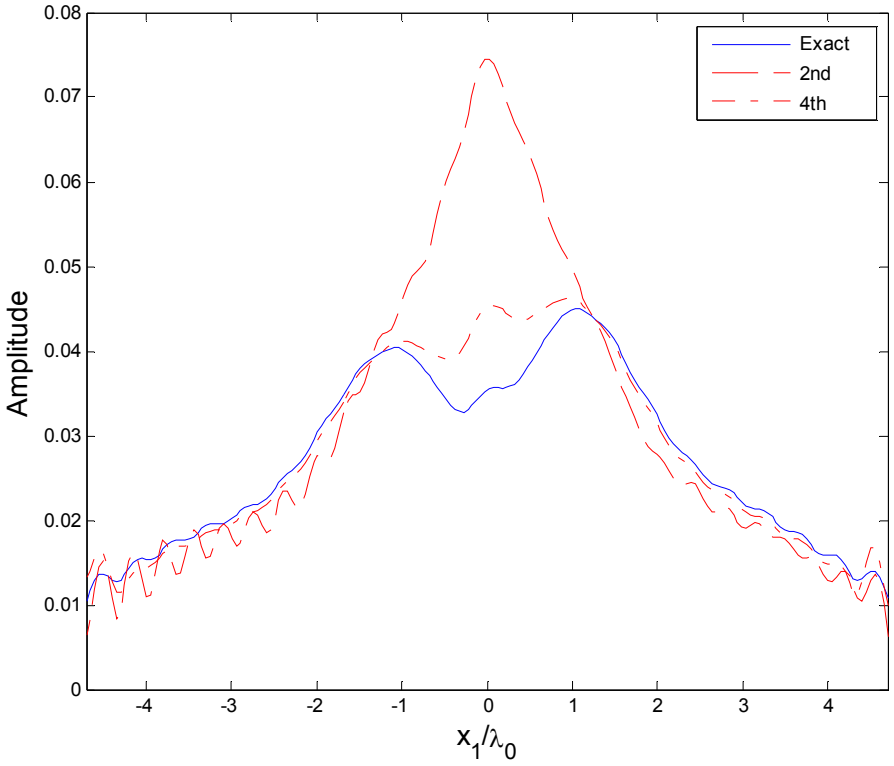

Figure 4.7 : Comparison of the fields at the lower boundary of the thin layer for Example 4.1.2

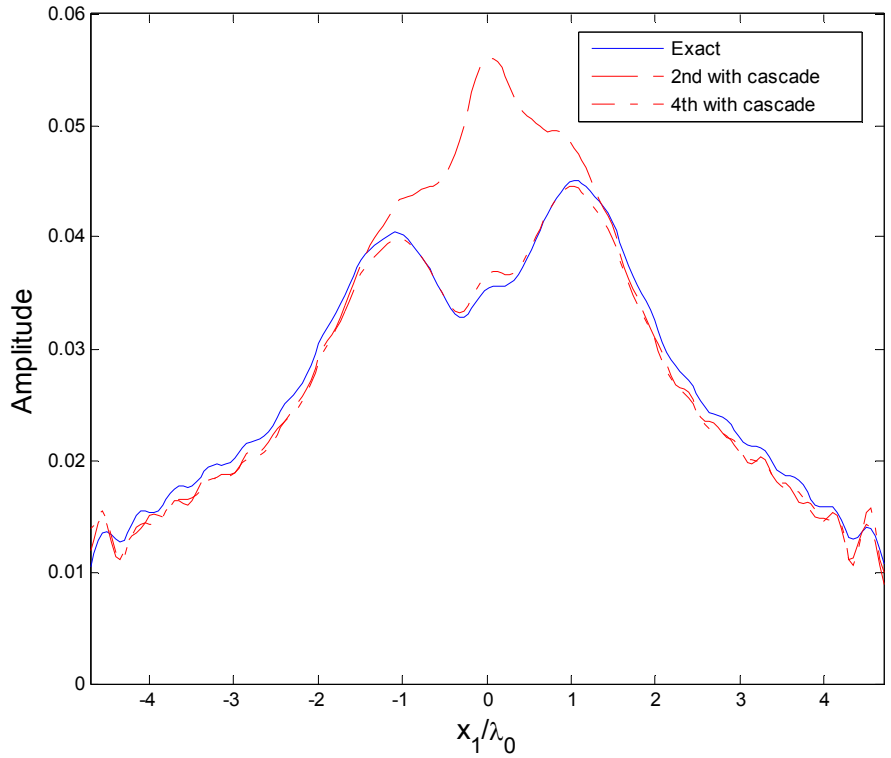

Figure 4.8 : Comparison of the fields at the lower boundary of the thin layer applying cascaded TLC for Example 4.1.2

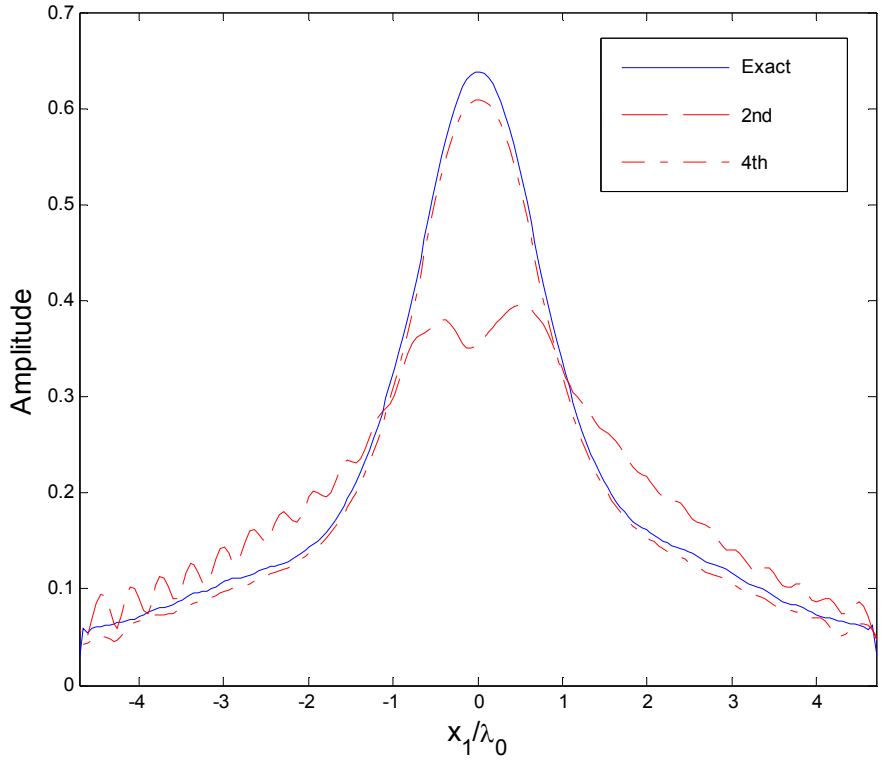

Figure 4.9 : Comparison of normal derivatives of the fields at the lower boundary of the thin layer for Example 4.1.2

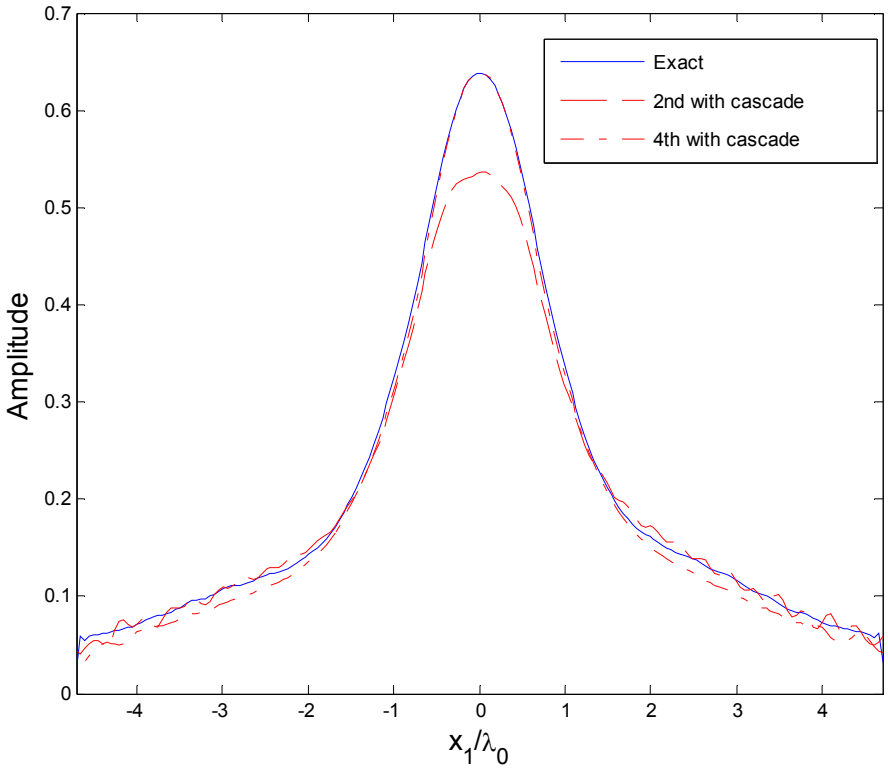

Figure 4.10 : Comparison of normal derivatives of the fields at the lower boundary of the thin layer applying cascaded TLC for Example 4.1.2

Figure 4.11 shows the reconstruction with exact data using RG-LSM.

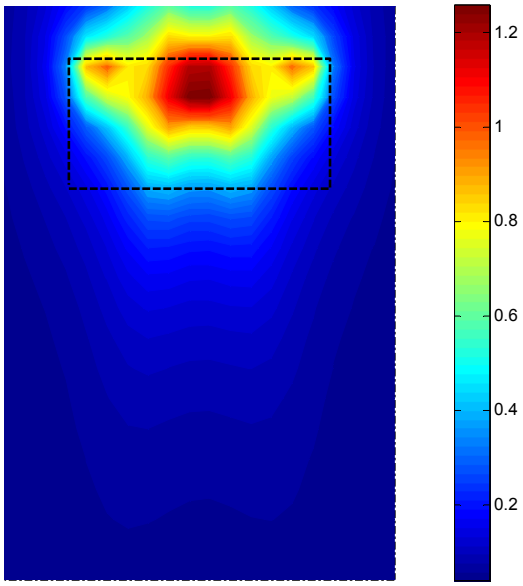

Figure 4.11 : Reconstruction associated with exact data for Example 4.1.2

The superiority of 4^{th} order TLC over 2^{nd} order TLC and the superiority of cascaded TLC over ordinary TLC can also be observed through the reconstruction figures, Figure 4.12, Figure 4.13, Figure 4.14 and Figure 4.15.

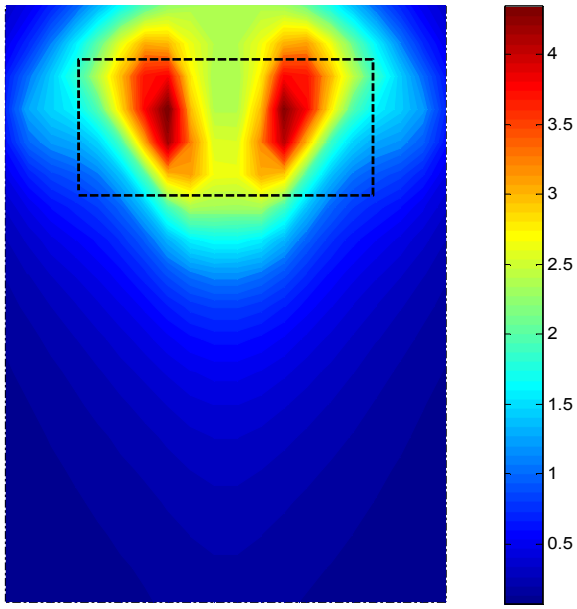

Figure 4.12 : Reconstruction associated with 2^{nd} order TLC for Example 4.1.2

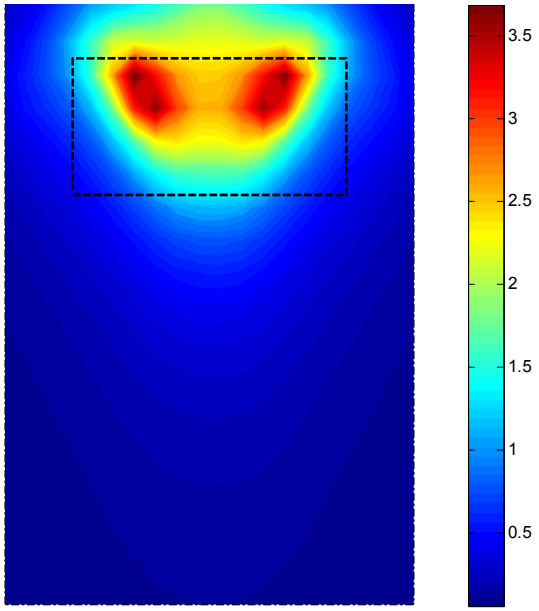

Figure 4.13 : Reconstruction associated with cascaded 2nd order TLC for Example 4.1.2

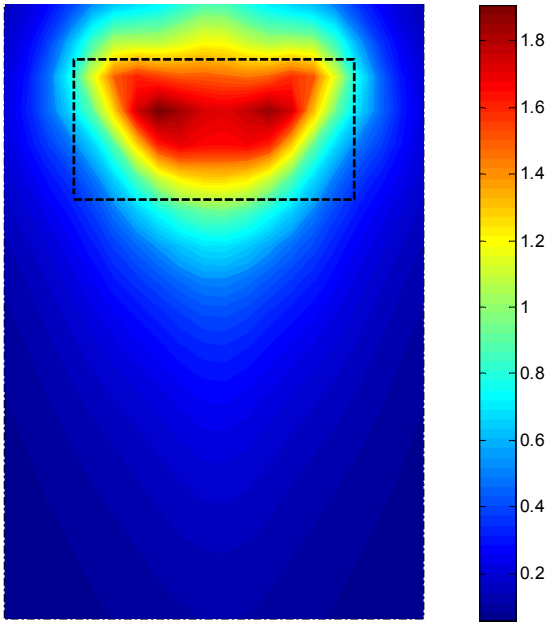

Figure 4.14 : Reconstruction associated with 4th order TLC for Example 4.1.2

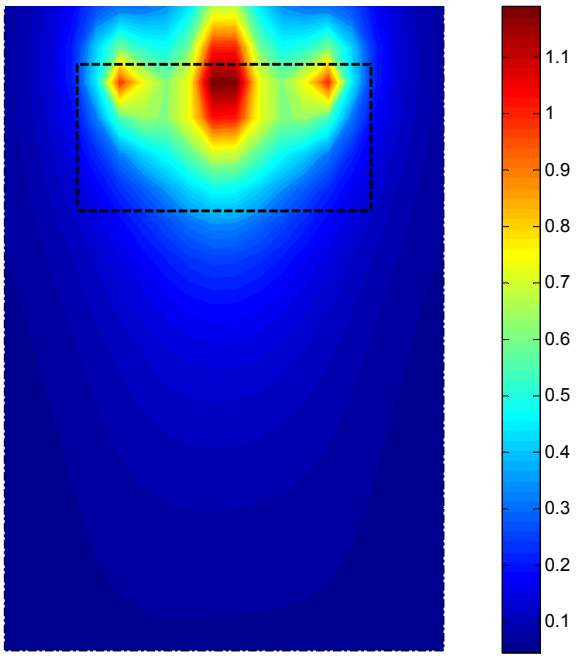

Figure 4.15 : Reconstruction associated with cascaded 4th order TLC for Example 4.1.2

Example 4.1.3. In the third example, we examined the effect of the relative permittivity of thin layer on TLC by increasing ε_{r_δ} from $2.5 + 0.2i$ to $6.0 + 0.2i$. Everything else stays the same as in Example 4.1.1. Figure 4.16 and Figure 4.17 show the comparison of field and its normal derivative. When we increase the relative permittivity of thin layer, the thin layer behaves like having larger thickness so, 4th order TLC gives better approximation than 2nd order TLC.

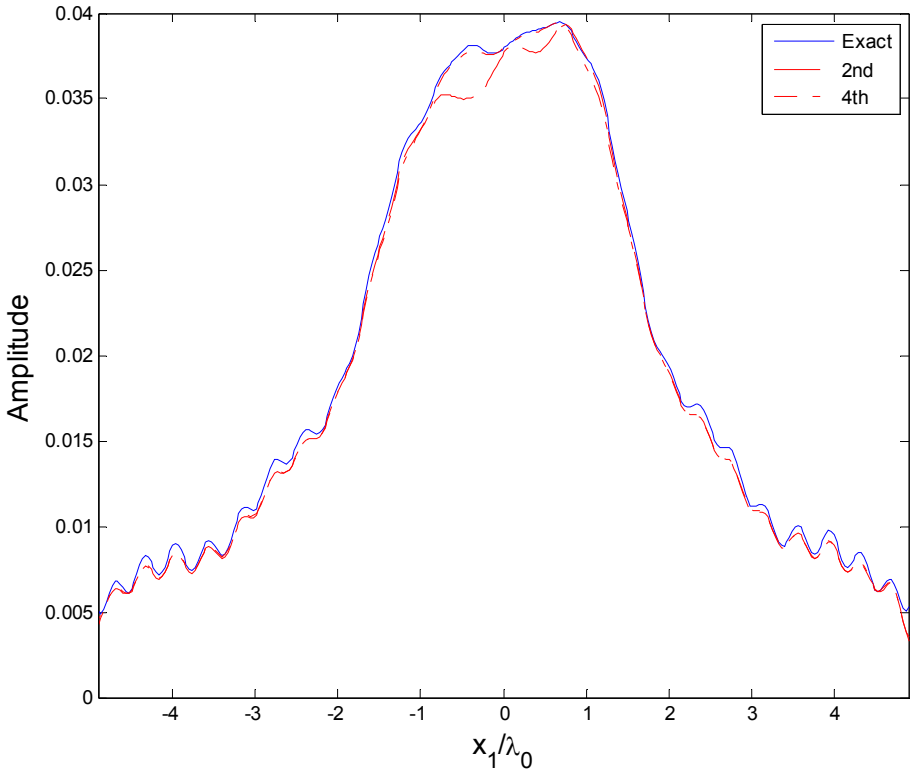

Figure 4.16 : Comparison of the fields at the lower boundary of the thin layer for Example 4.1.3

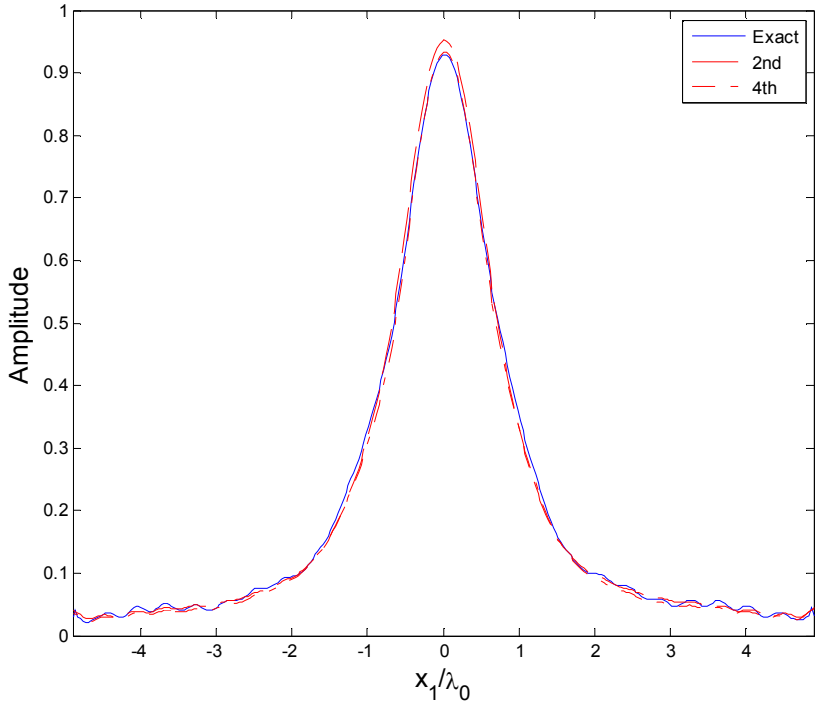

Figure 4.17 : Comparison of normal derivatives of the fields at the lower boundary of the thin layer for Example 4.1.3

We can see this superiority also at reconstruction figures, Figure 4.18, Figure 4.19, Figure 4.20.

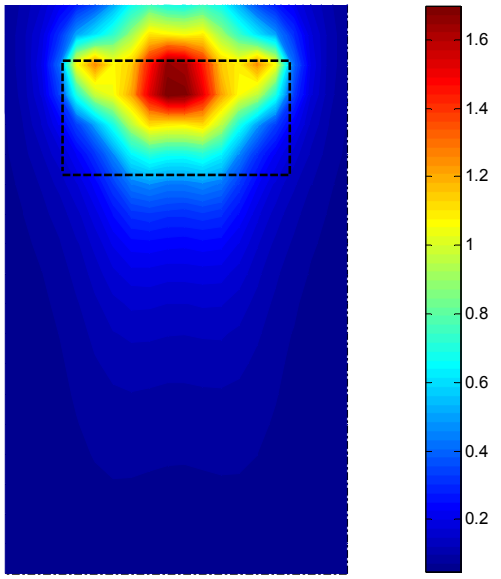

Figure 4.18 : Reconstruction associated with exact data for Example 4.1.3

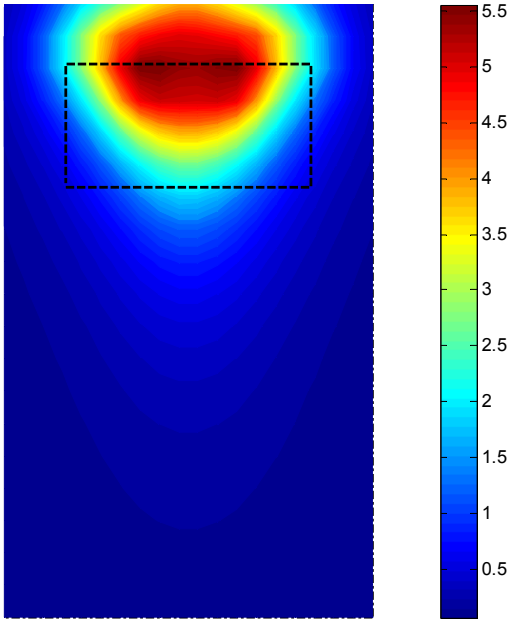

Figure 4.19 : Reconstruction associated with 2nd order TLC for Example 4.1.3

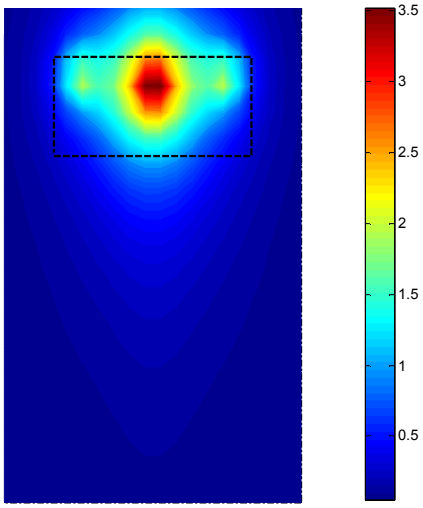

Figure 4.20 : Reconstruction associated with 4th order TLC for Example 4.1.3

In order to make precise comparison, an error function is defined as $\frac{\|U_{EXACT}-U_{APP}\|^2}{\|U_{EXACT}\|^2}$.

To show the relation between relative permittivity of thin layer and accuracy of approximation of fields, Figure 4.21 and Figure 4.22 are plotted. As we mentioned it earlier, error increases while relative permittivity becomes larger. Another issue is that 4th order TLC is less sensible to dielectric constant than 2nd order TLC.

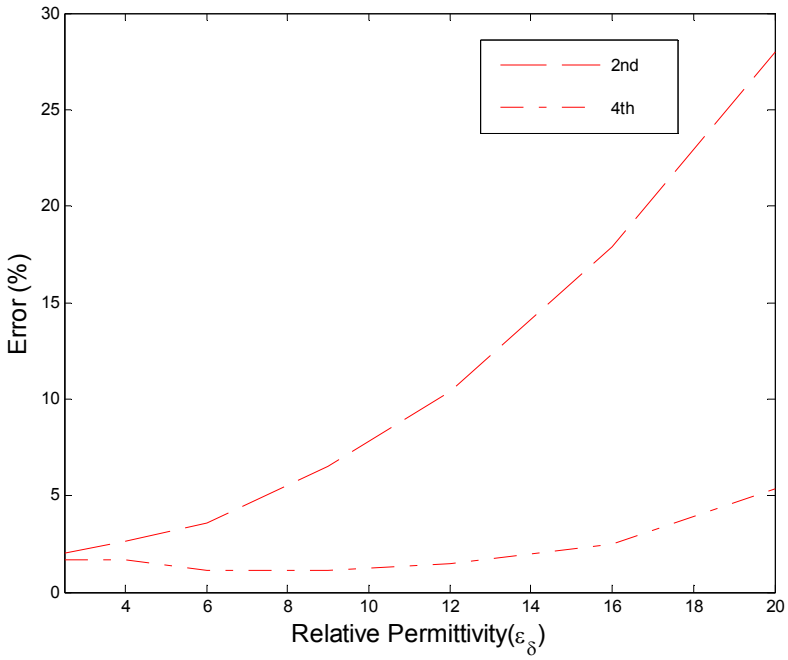

Figure 4.21 : Error for field calculation versus a relative permittivity of thin layer

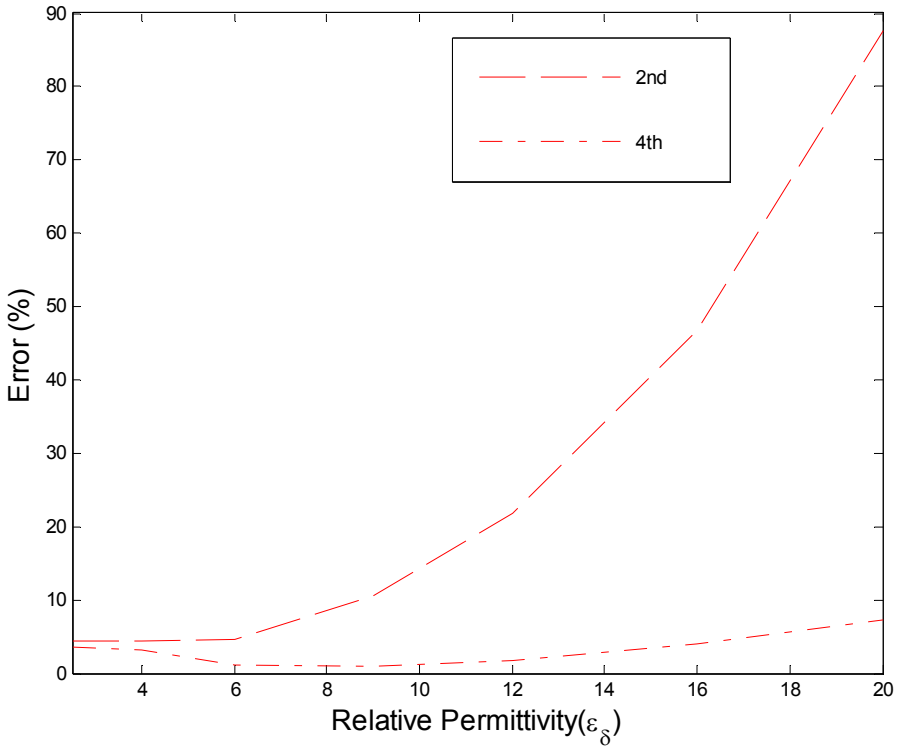

Figure 4.22 : Error for normal derivative of field calculation versus a relative permittivity of thin layer

Example 4.1.4. The fourth example is presented to show that thin layer approximation is also valid for multi-layered medium. In this example, two different thin layers are placed between air and the medium where the object is buried. The upper thin layer has a relative permittivity as $\varepsilon_{r_{\delta 1}} = 3.0 + 0.2i$ and the relative permittivity of the lower one is $\varepsilon_{r_{\delta 2}} = 2.5 + 0.2i$. The thickness of both layers is equal to $0.1\lambda_0$. Perfectly conducting rectangle-shaped object with dimensions $\lambda_0 \times \lambda_0/2$ is buried in a lowest homogeneous medium with relative permittivity $\varepsilon_r = 1.5 + 0.2i$.

Comparison of approximated and exact field and normal derivative of the field are given Figure 4.23 and Figure 4.24, respectively. It is obvious from figures that thin layer condition is feasible for thin layer comprised of multi layers. As it is expected, 4th TLC gives better result than 2nd order TLC.

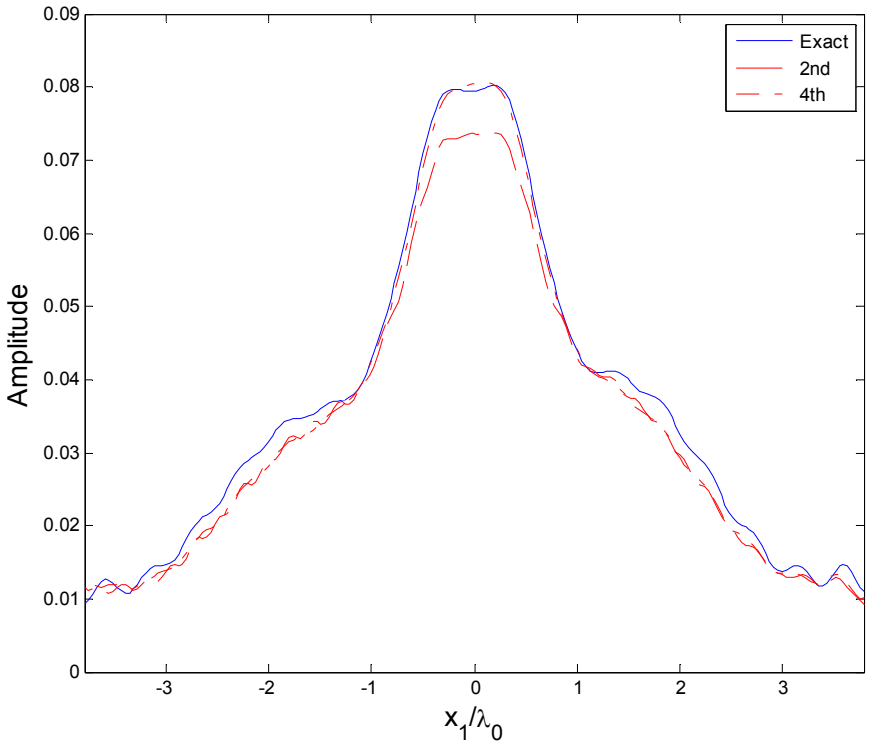

Figure 4.23 : Comparison of the fields at the lower boundary of the lower thin layer for Example 4.1.4

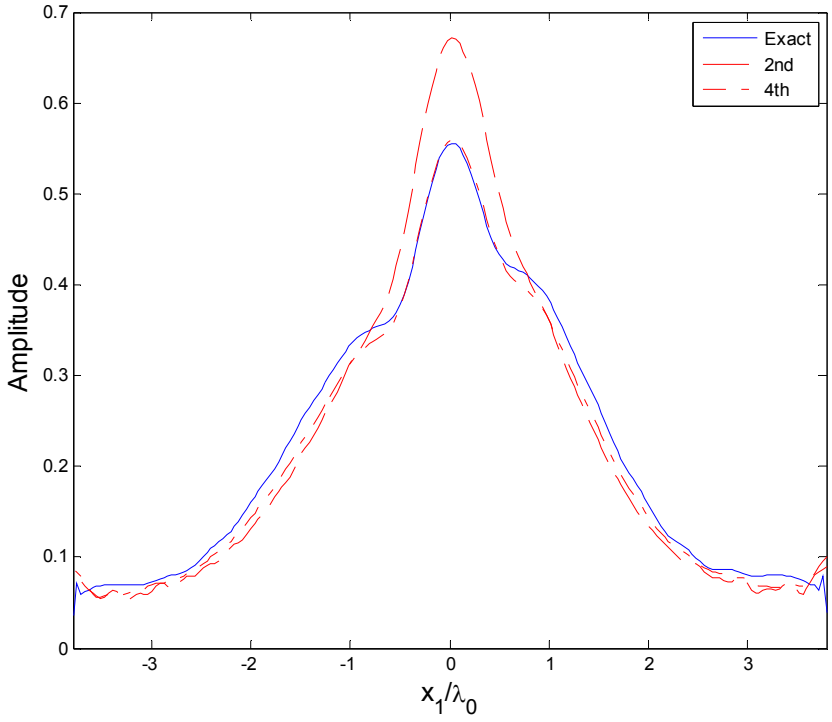

Figure 4.24 : Comparison of normal derivatives of the fields at the lower boundary of the lower thin layer for Example 4.1.4

Reconstructions done by RG-LSM are shown in Figure 4.25, Figure 4.26, Figure 4.27.

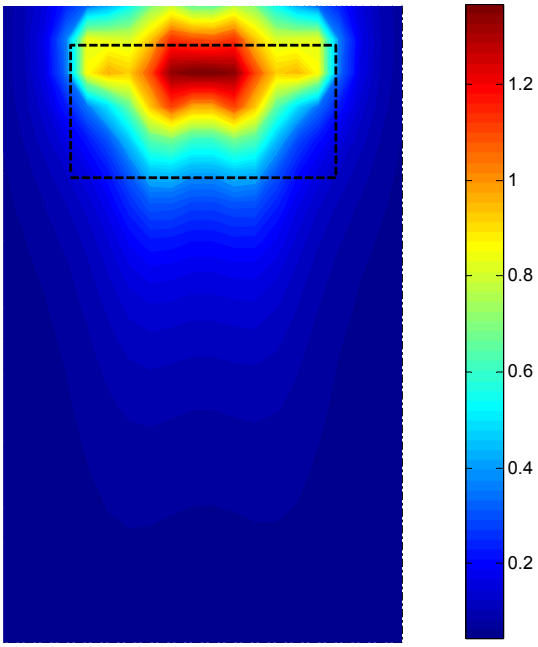

Figure 4.25 : Reconstruction associated with exact data for Example 4.1.4

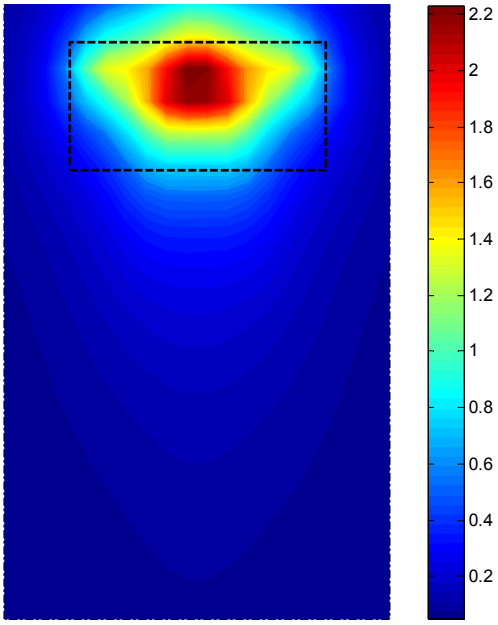

Figure 4.26 : Reconstruction associated with 2nd order TLC for Example 4.1.4

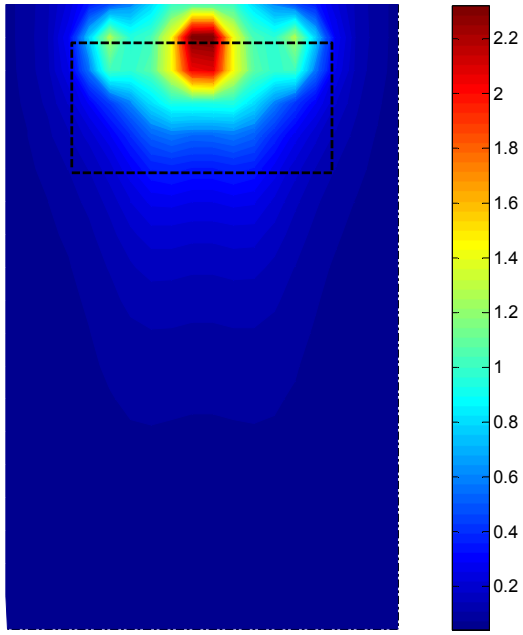

Figure 4.27 : Reconstruction associated with 4^{th} order TLC for Example 4.1.4

4.2. Numerical Results For Rough Interfaces

Second part of numerical results section is devoted for rough interfaced medium. In this case, curvature term and derivative of curvature term should be taken into account in Equations (2.46-2.51), therefore the solution of equations becomes more difficult.

General geometry and parameters for rough interface case are shown in Figure 4.28.

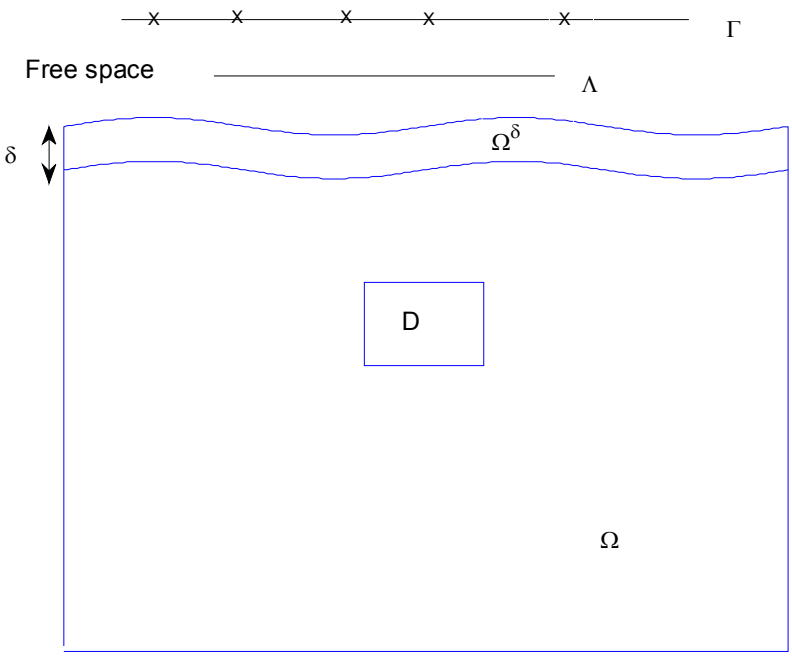

Figure 4.28 : General structure of the problem in rough case

$\Gamma, D, \Omega, \Omega^{\delta}, \delta$ and Λ symbolize same things as given in flat interface section.

Example 4.2.1. In the first example, thin layer is placed between free space and homogeneous media with $\varepsilon_r = 1.5 + 0.2i$. Thickness of the thin layer is chosen as $\delta = 0.1\lambda_0$ and relative permittivity of the thin layer is chosen as $\varepsilon_{r_\delta} = 2.5 + 0.2i$. Perfectly conducting rectangle-shaped object with dimensions $\lambda_0 \times \lambda_0/2$ is buried in a lower homogeneous medium. All exciting sources are located in only upper part. Roughness of surface is chosen as sinusoidal and defined by $y = 0.1 \sin\frac{\pi x}{2}$. Notice that peak to peak value of its amplitude is $0.2\lambda_0$.

Figure 4.29 and Figure 4.30 show the comparison of the field and its normal derivative at the lower boundary of the thin layer, respectively. As for flat interfaced layer having $\delta = 0.1\lambda_0$ thickness, there is almost no difference between approximated fields obtained by using 2nd and 4th order TLC. However, because of non-zero curvature term, accuracy of thin layer condition is worse than the Example 4.1.1.

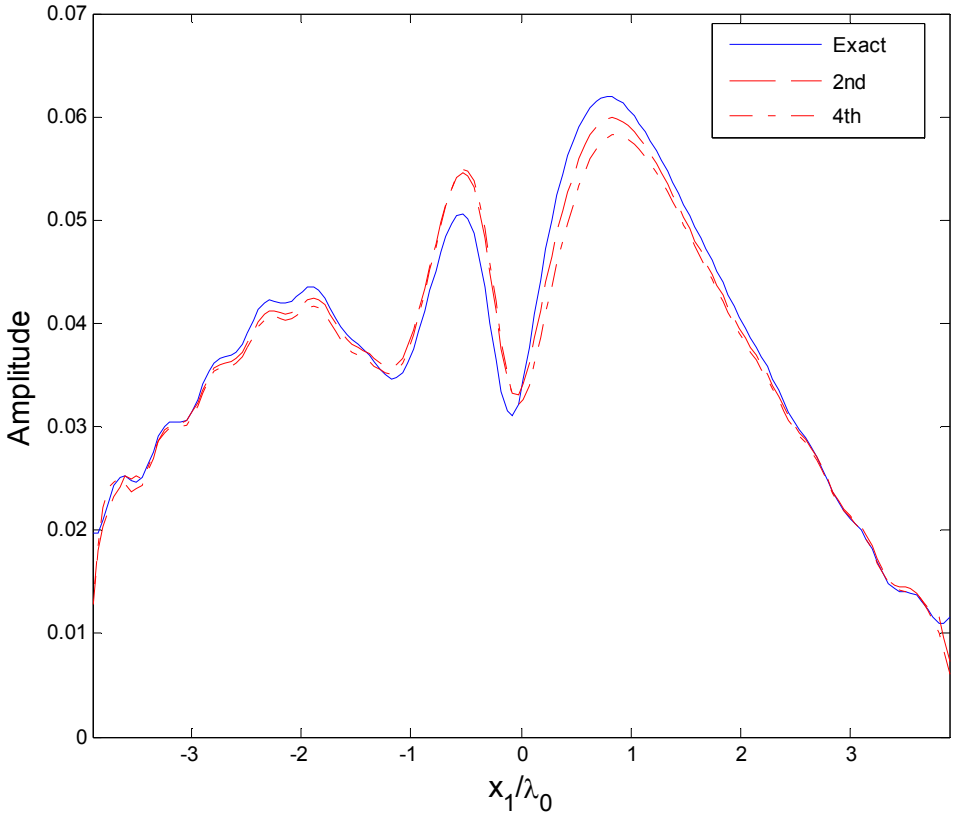

Figure 4.29 : Comparison of the fields at the lower boundary of the thin layer for Example 4.2.1

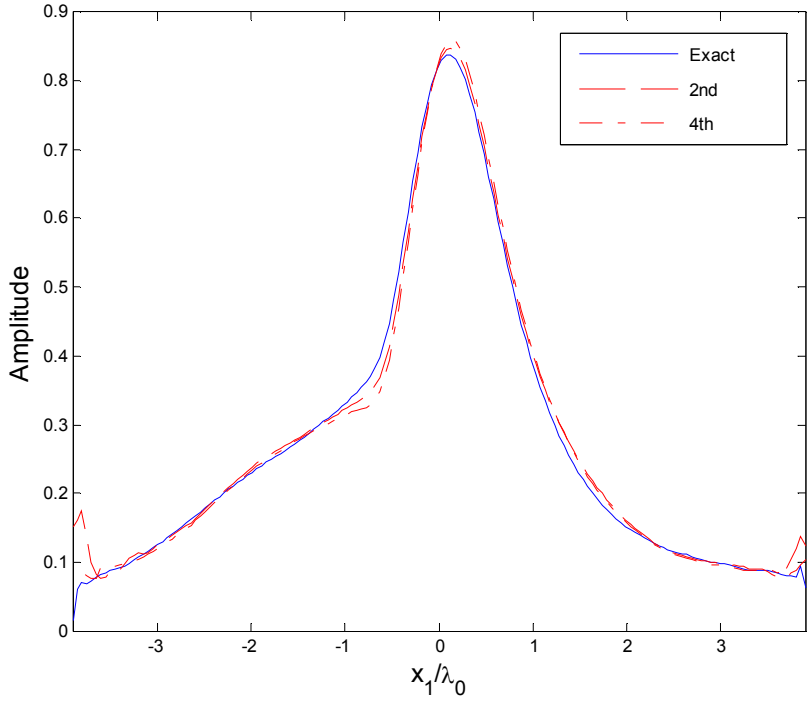

Figure 4.30 : Comparison of normal derivatives of the fields at the lower boundary of the thin layer for Example 4.2.1

Then, reconstructions of the object with exact data and data obtained by 2^{nd} and 4^{th} order TLC are shown in Figure 4.31, Figure 4.32 and Figure 4.33, respectively and they prove that reconstruction of the object can be done successfully by using approximated data.

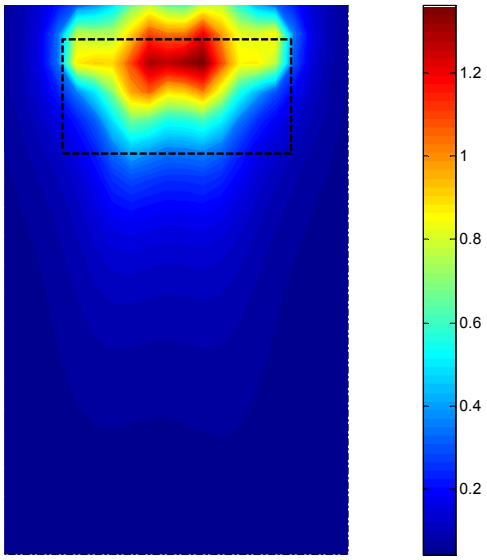

Figure 4.31 : Reconstruction associated with exact data for Example 4.2.1

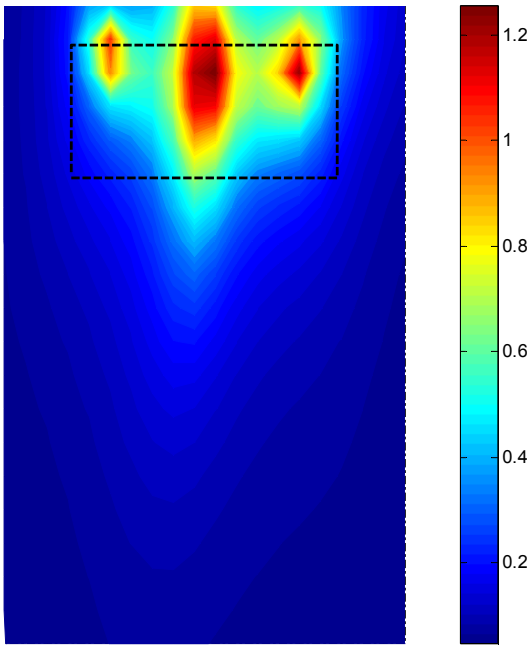

Figure 4.32 : Reconstruction associated with 2nd order TLC for Example 4.2.1

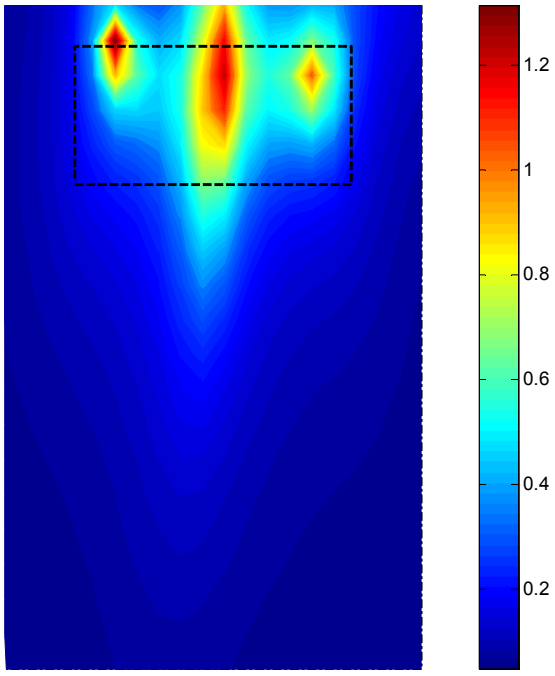

Figure 4.33 : Reconstruction associated with 4th order TLC for Example 4.2.1

Example 4.2.2. The second example is done to see the effect of roughness. For this purpose, while keeping the thickness $\delta = 0.1\lambda_0$ (same as in Example 4.2.1), we have changed the peak to peak amplitude of roughness from $0.2\lambda_0$ to $0.6\lambda_0$. The other parameters are same as Example 4.2.1.

As it is expected because of big roughness, approximation of the fields and its normal derivative are worse than the previous example, see Figure 4.34 and Figure 4.35.

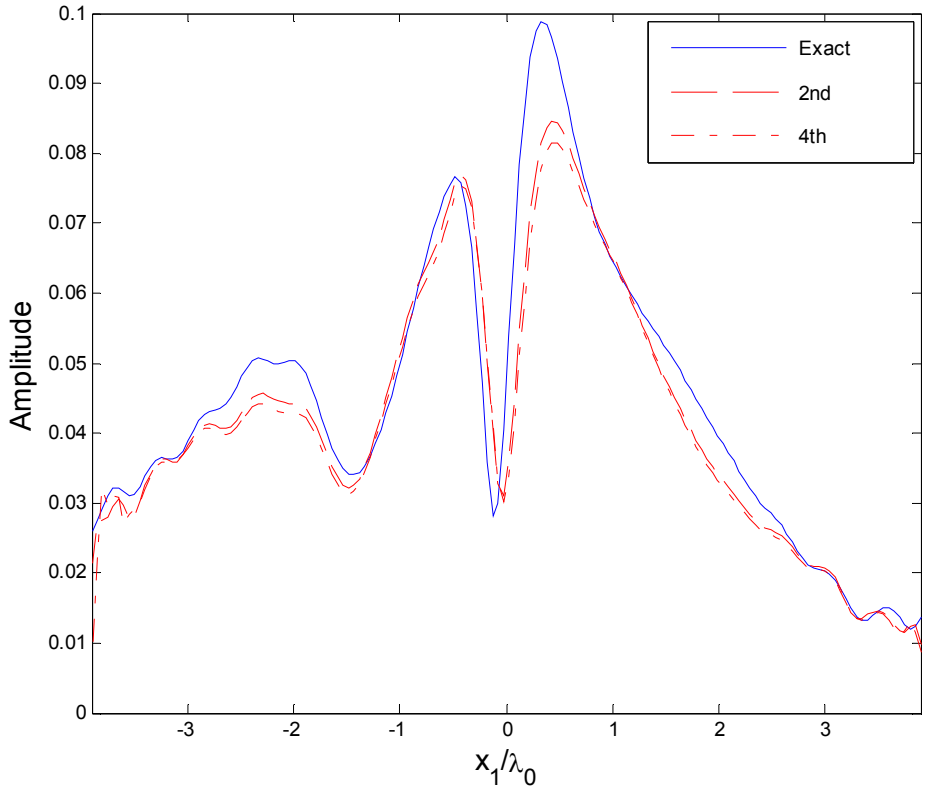

Figure 4.34 : Comparison of the fields at the lower boundary of the thin layer for Example 4.2.2

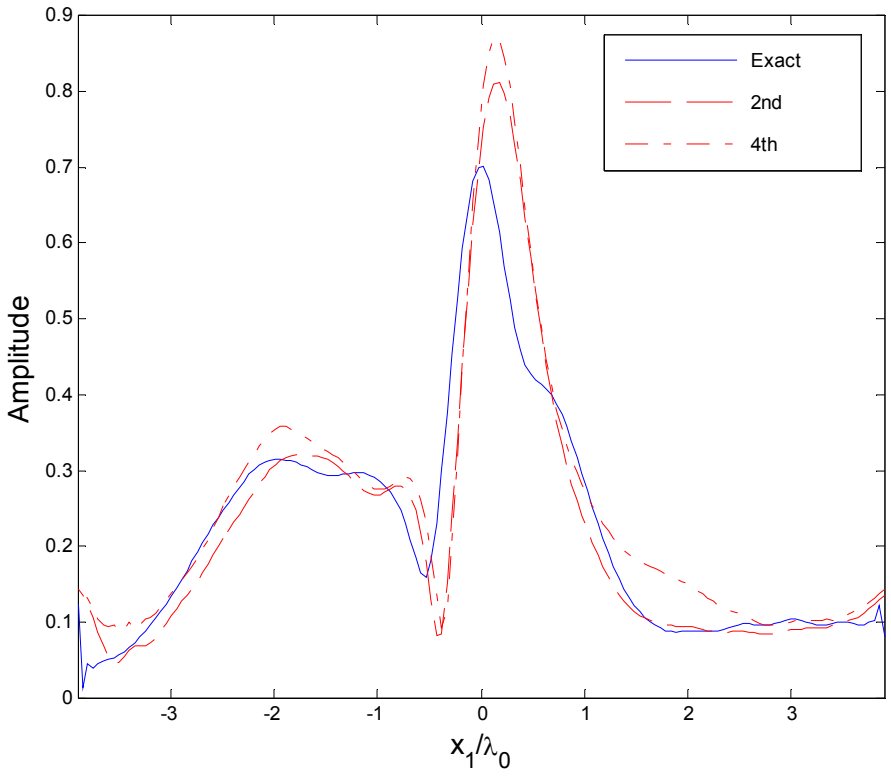

Figure 4.35 : Comparison of normal derivatives of the fields at the lower boundary of the thin layer for Example 4.2.2

This effect can be seen clearly also on reconstruction of the object done by approximated fields, see Figure 4.36, Figure 4.37 and Figure 4.38.

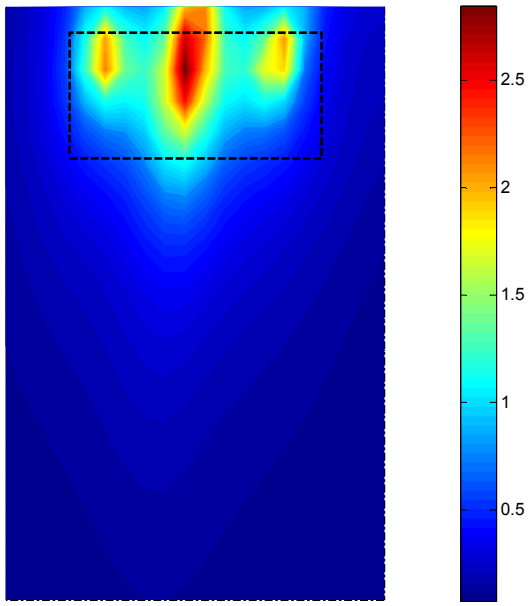

Figure 4.36 : Reconstruction associated with exact data for Example 4.2.2

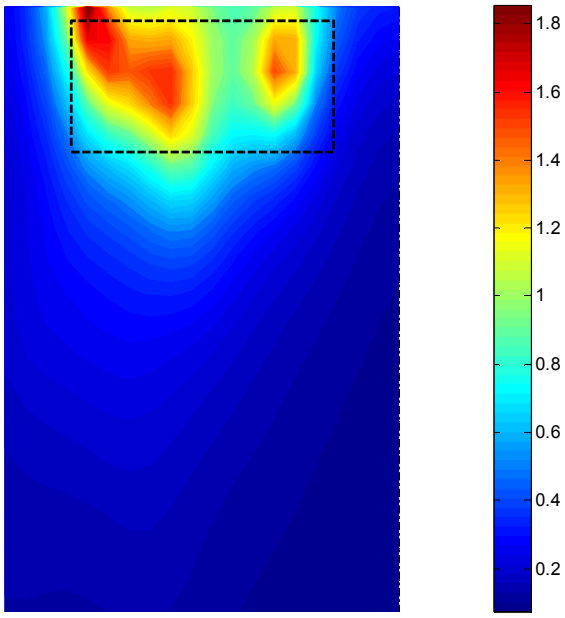

Figure 4.37 : Reconstruction associated with 2nd order TLC for Example 4.2.2

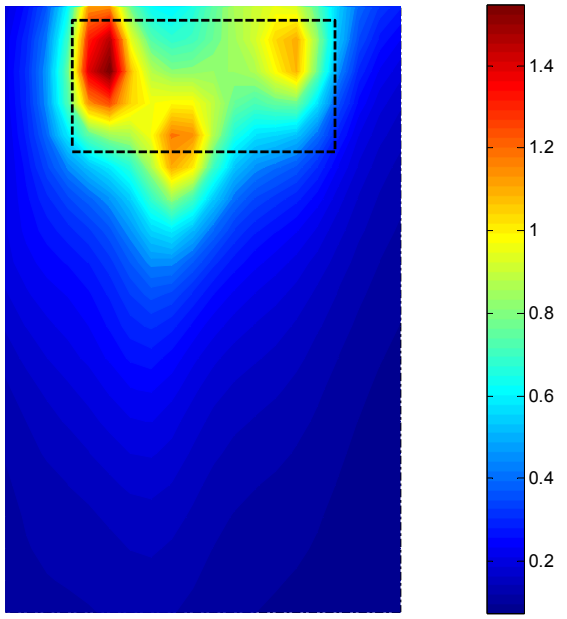

Figure 4.38 : Reconstruction associated with 4th order TLC for Example 4.2.2

Example 4.2.3. With this example, as it is done for flat interfaced layers, we want to show that thin layer approximation can be applied to multi layers having rough interface and its roughness profile is defined by $y = 0.1 \sin\frac{\pi x}{2}$. 2 thin layers, each one having $0.15\lambda_0$ thickness, are placed between the air and the medium where the object is buried. Relative permittivity of the upper thin layer is chosen with $\varepsilon_{r_{\delta 1}} = 2.5 + 0.2i$ and the lower thin layer is chosen with $\varepsilon_{r_{\delta 2}} = 2.0 + 0.2i$. Perfectly conducting rectangle-shaped object with dimensions $\lambda_0 \times \lambda_0/2$ is buried in a lower homogeneous medium with $\varepsilon_r = 1.5 + 0.2i$.

Figure 4.39 and Figure 4.40 show the comparison of field and its normal derivative. As it is expected, 4th order TLC gives much better approximation than 2nd order TLC.

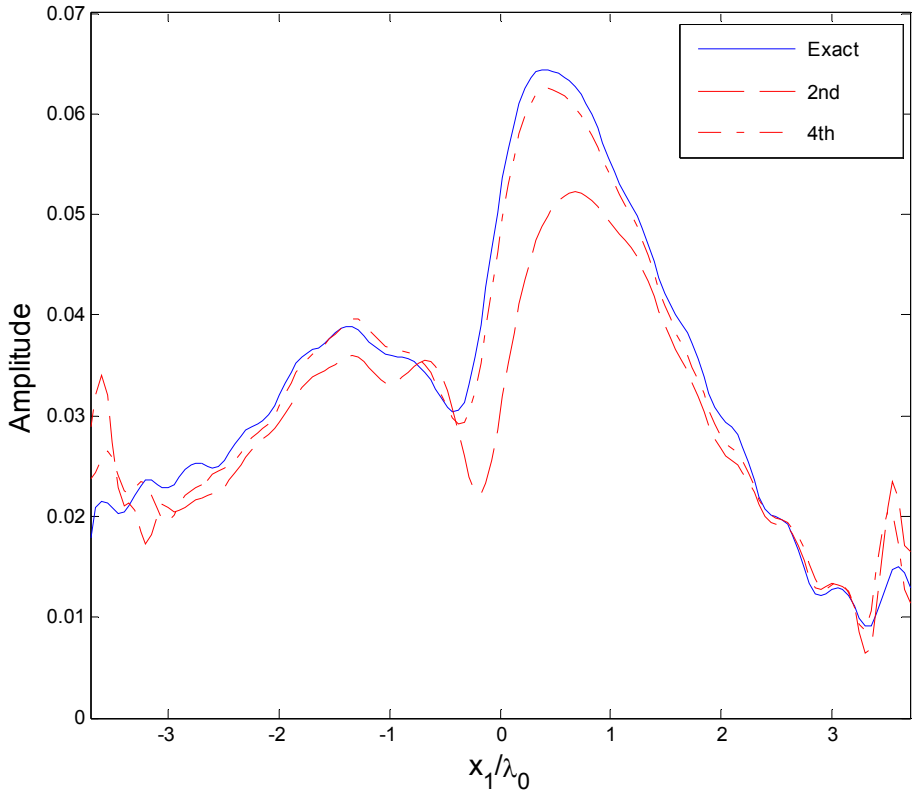

Figure 4.39 : Comparison of the fields at the lower boundary of the lower thin layer for Example 4.2.3

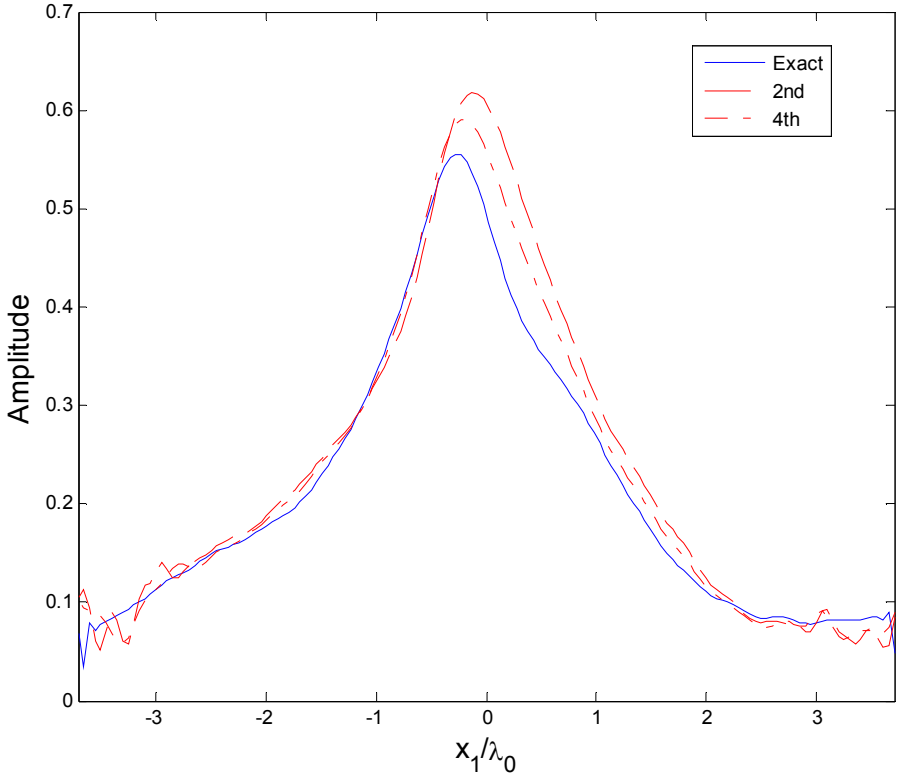

Figure 4.40 : Comparison of normal derivatives of the fields at the lower boundary of the lower thin layer for Example 4.2.3

Then, reconstructions of the object with exact data and data obtained by 2^{nd} and 4^{th} order TLC are done and presented in Figure 4.41, Figure 4.42 and Figure 4.43, respectively.

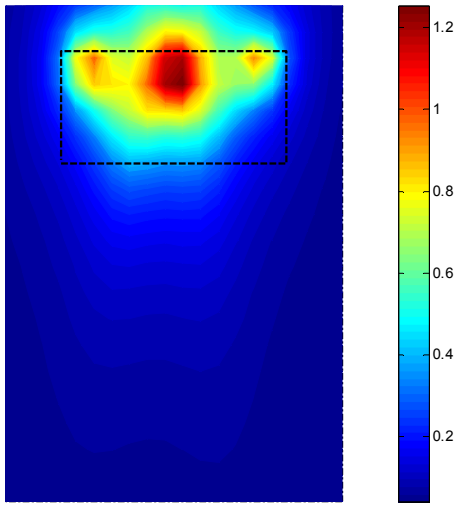

Figure 4.41 : Reconstruction associated with exact data for Example 4.2.3

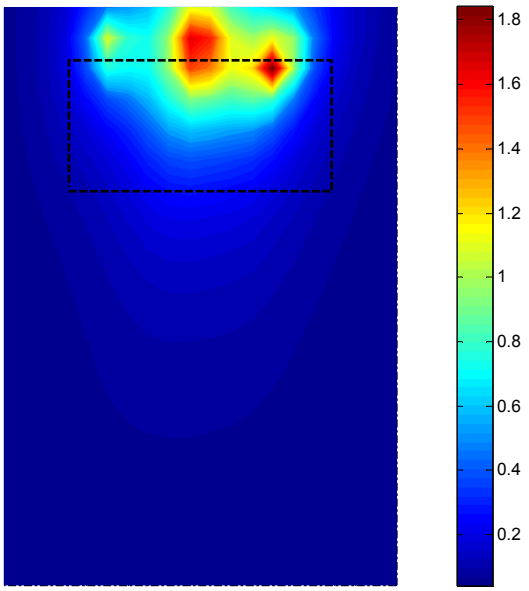

Figure 4.42 : Reconstruction associated with 2nd order TLC for Example 4.2.3

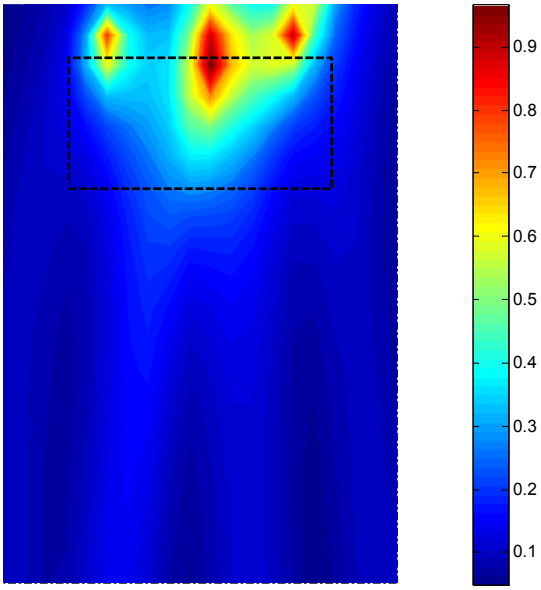

Figure 4.43 : Reconstruction associated with 4th order TLC for Example 4.2.3

4.3. Numerical Results For Circular Interfaces

Final part of numerical results section is devoted to cylindrical medium with circular cross-section. In circular cross-section case, curvature term in thin layer approximations is taken into account and is equal to $\frac{1}{R}$ where R is the radius of circle.

General geometry and parameters for circular interface case are shown in Figure 4.44

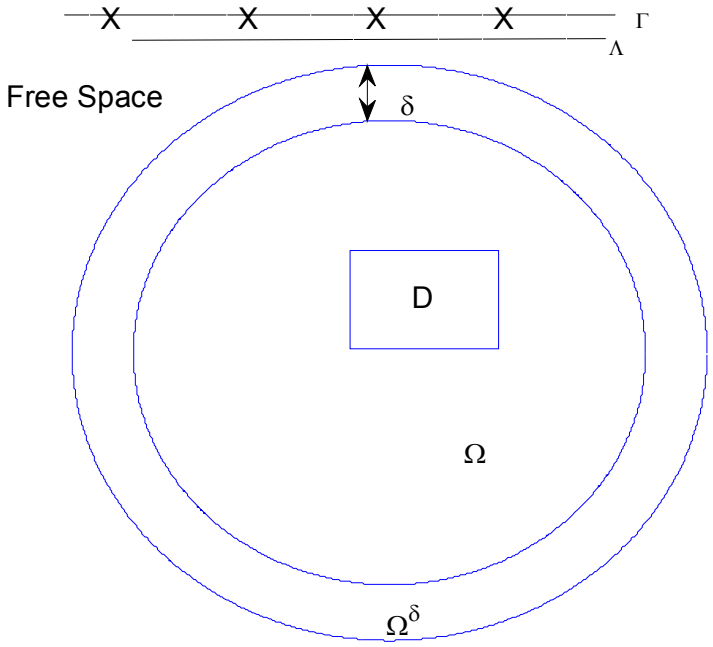

Figure 4.44 : General structure of the problem in cylindrical medium

$\Gamma, D, \Omega, \Omega^{\delta}, \delta$ and Λ symbolize same things as given in flat interface section.

Example 4.3.1. In the first example, thin layer is placed between free space and homogeneous media with $\varepsilon_r = 1.5 + 0.2i$. Thickness of the thin layer is chosen as $\delta = 0.1\lambda_0$ and relative permittivity of the thin layer is chosen as $\varepsilon_{r_\delta} = 6.0 + 0.2i$. Perfectly conducting rectangle-shaped object with dimensions $\lambda_0 \times \lambda_0/2$ is buried in a lower homogeneous medium. All exciting sources are located in only upper part. The field and its normal derivative at the lower boundary of the thin layer are approximated with 2nd and 4th order thin layer conditions and comparison of them with exact field are given Figure 4.45 and Figure 4.46, respectively. As it is expected, 4th order TLC gives better approximation than 2nd order TLC because of higher dielectric constant of the layer.

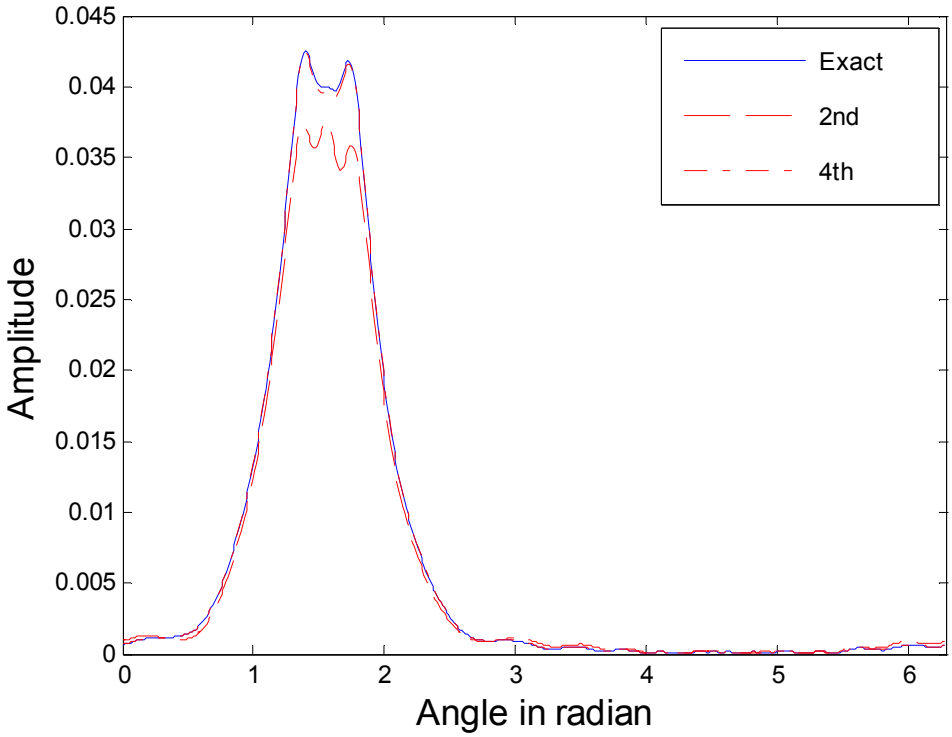

Figure 4.45 : Comparison of the fields at the lower boundary of the thin layer for Example 4.3.1

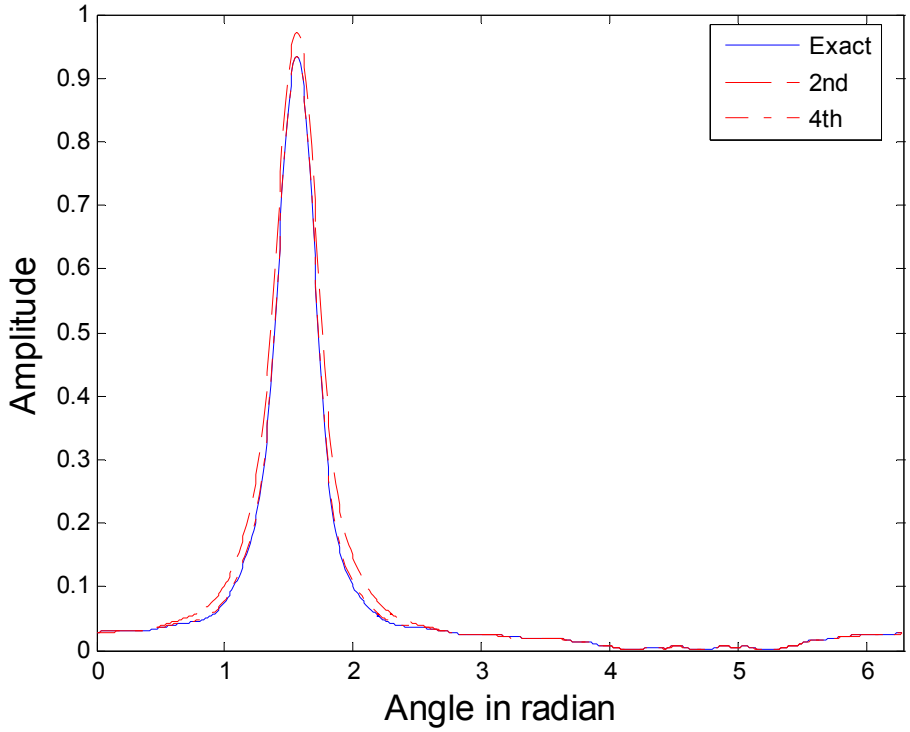

Figure 4.46 : Comparison of normal derivatives of the fields at the lower boundary of the thin layer for Example 4.3.1

Then, reconstructions of the object with exact data and data obtained by 2^{nd} and 4^{th} order TLC are done and presented in Figure 4.47, Figure 4.48 and Figure 4.49, respectively.

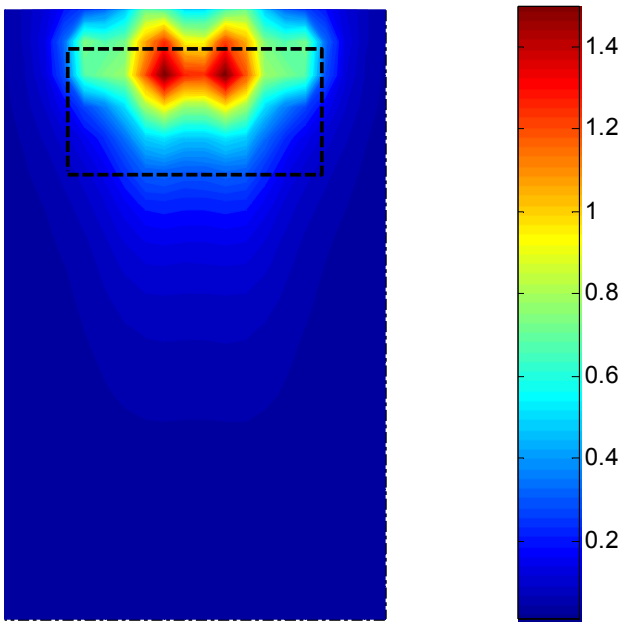

Figure 4.47 : Reconstruction associated with exact data for Example 4.3.1

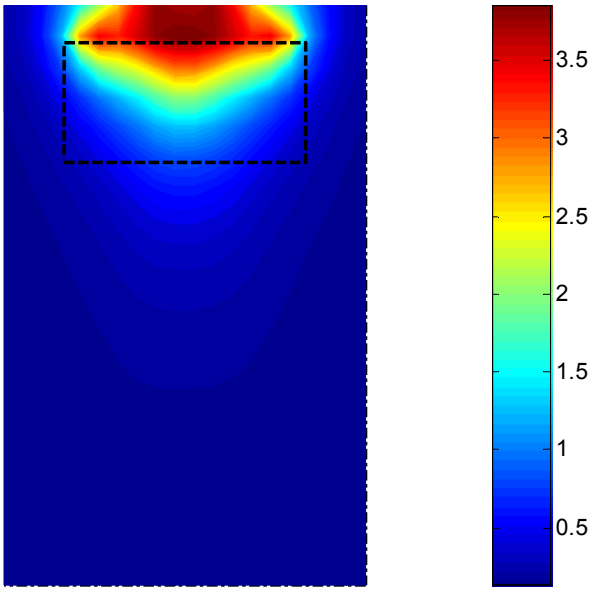

Figure 4.48 : Reconstruction associated with 2^{nd} order TLC for Example 4.3.1

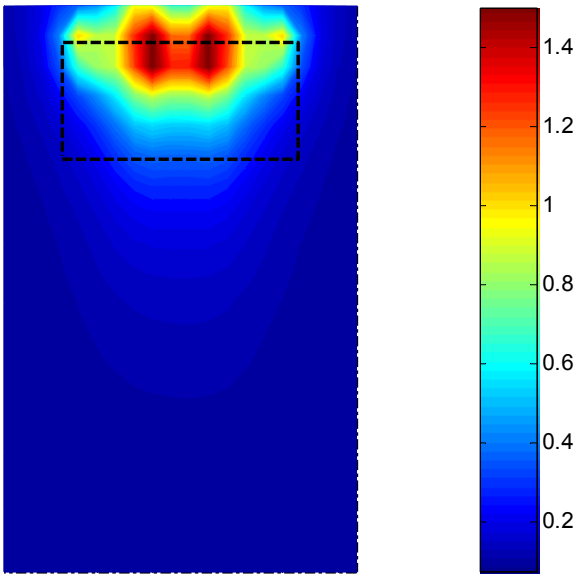

Figure 4.49: Reconstruction associated with 4th order TLC for Example 4.3.1

Example 4.3.2 The second example is done to see the effect of thickness. With this aim, δ is increased from $0.1\lambda_0$ to $0.3\lambda_0$. Everthing else stays the same as in example 4.3.1. Figure 4.50 and Figure 4.52 show the comparison of field and its normal derivative. As it is expected, when the thickness is large, 4th order TLC gives much better approximation than 2nd order TLC. However, even 4th order TLC does not approximate the exact field as good as the case 4.3.1 which is done for $\delta = 0.1\lambda_0$. The reason for this is that accuracy of the TLC depends on thickness, δ, see Equations (2.46-2.51). Therefore to improve our result, we assume that this large thickness, $\delta = 0.3\lambda_0$ can be thought of combination of two same layers with thickness, $\delta_{1,2} = 0.15\lambda_0$ and we applied cascaded thin layer conditions two times. With cascaded 4th order TLC, even for larger thickness, almost the exact field values are obtained, see Figure 4.51 and Figure 4.53.

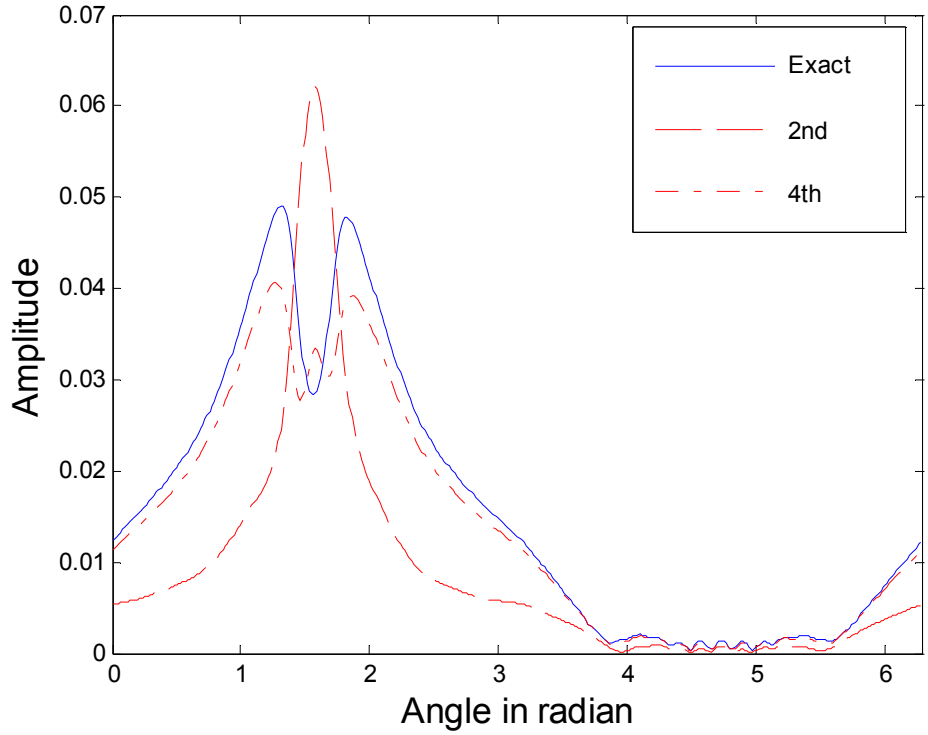

Figure 4.50 : Comparison of the fields at the lower boundary of the thin layer for Example 4.3.2

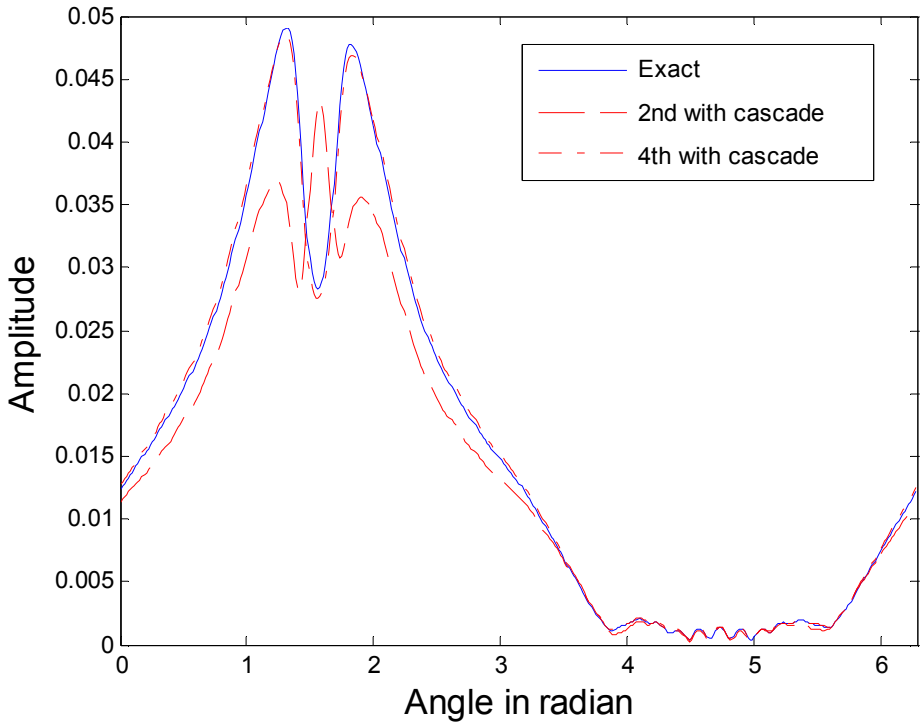

Figure 4.51 : Comparison of the fields at the lower boundary of the thin layer applying cascaded TLC for Example 4.3.2

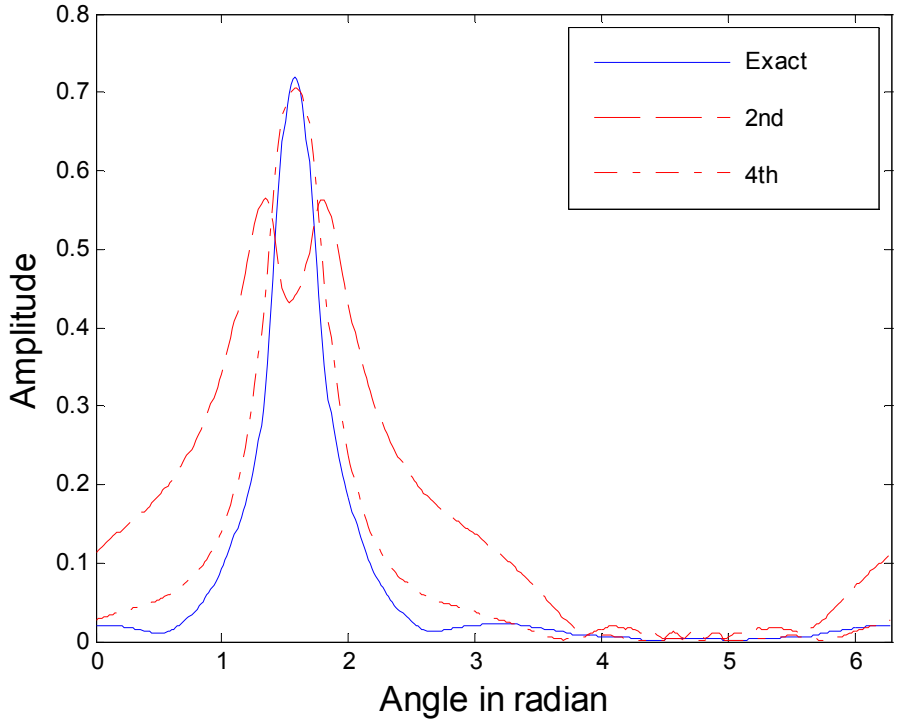

Figure 4.52 : Comparison of normal derivatives of the fields at the lower boundary of the thin layer for Example 4.3.2

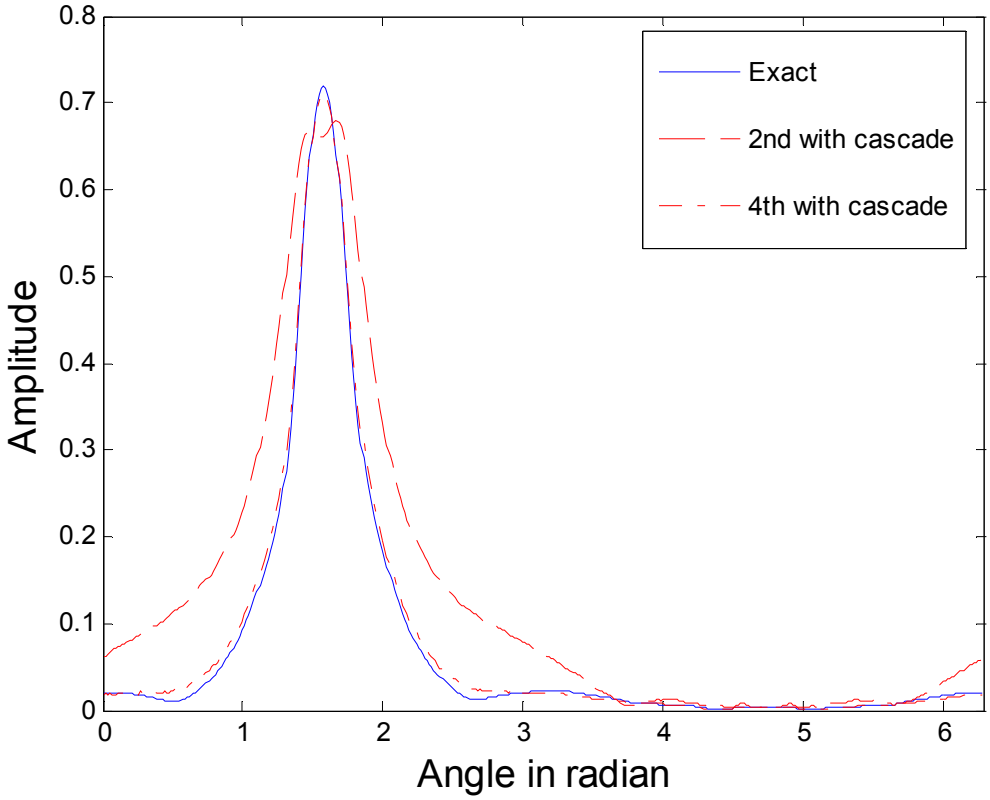

Figure 4.53 : Comparison of normal derivatives of the fields at the lower boundary of the thin layer applying cascaded TLC for Example 4.3.2

Figure 4.54 shows the reconstruction with exact data using RG-LSM.

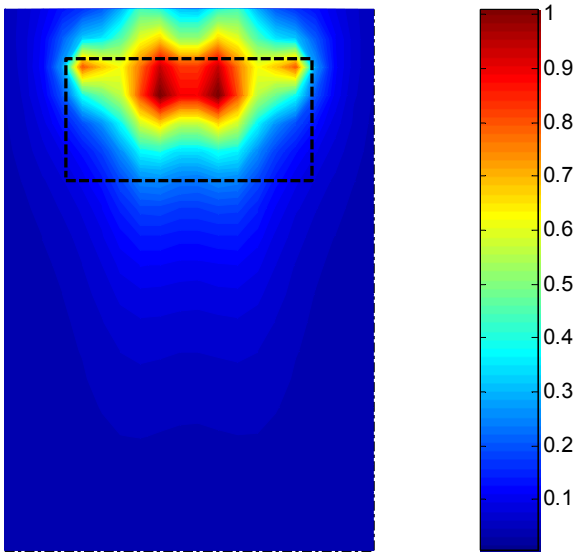

Figure 4.54 : Reconstruction associated with exact data for Example 4.3.2

The superiority of 4^{th} order TLC over 2^{nd} order TLC and the superiority of cascaded TLC over ordinary TLC can be also observed through the reconstruction figures, Figure 4.55, Figure 4.56, Figure 4.57 and Figure 4.58.

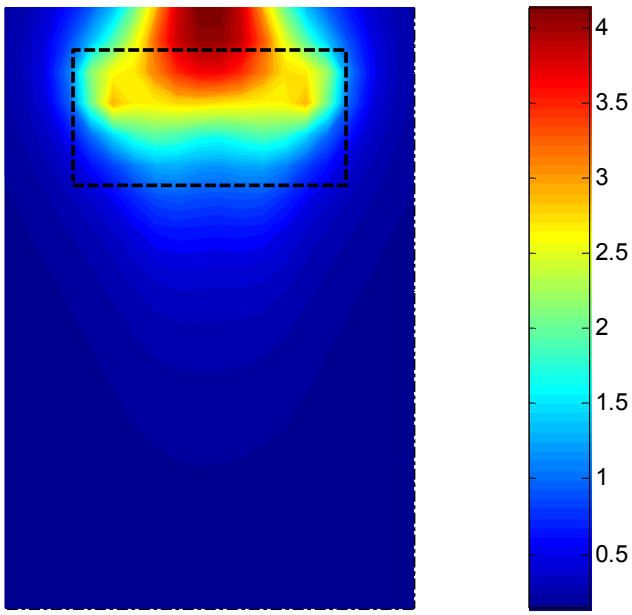

Figure 4.55 : Reconstruction associated with 2^{nd} order TLC for Example 4.3.2

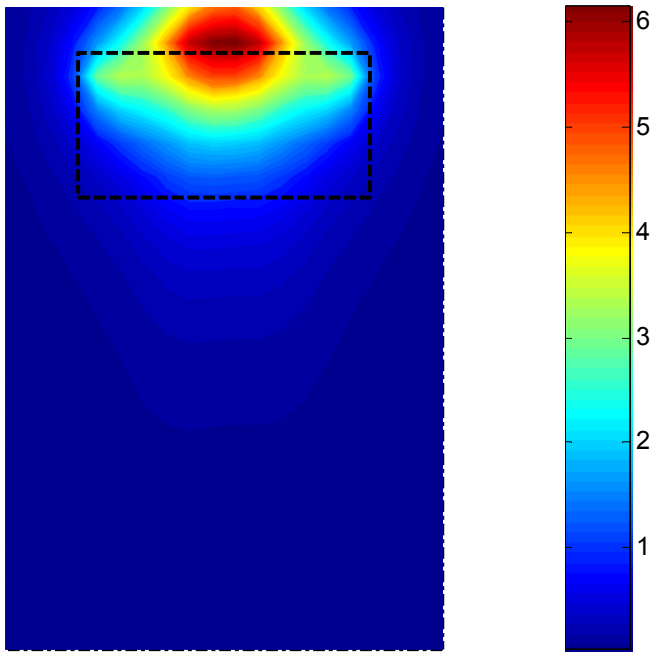

Figure 4.56 : Reconstruction associated with cascaded 2nd order TLC for Example 4.3.2

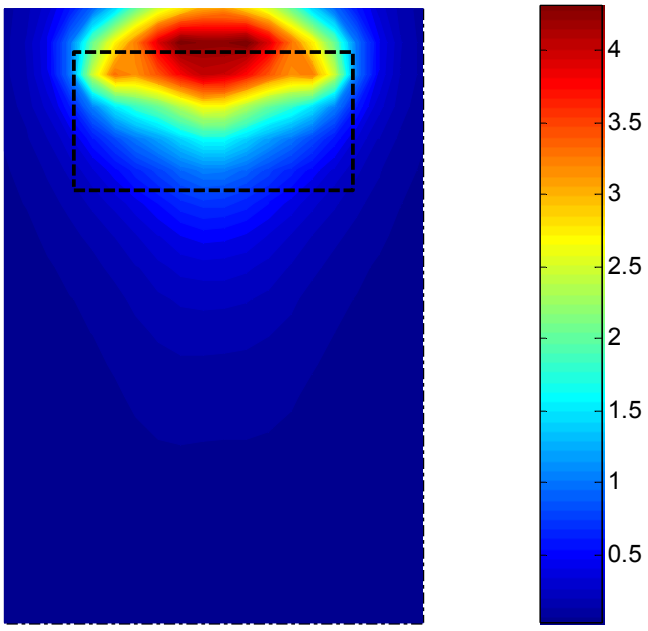

Figure 4.57 : Reconstruction associated with 4th order TLC for Example 4.3.2

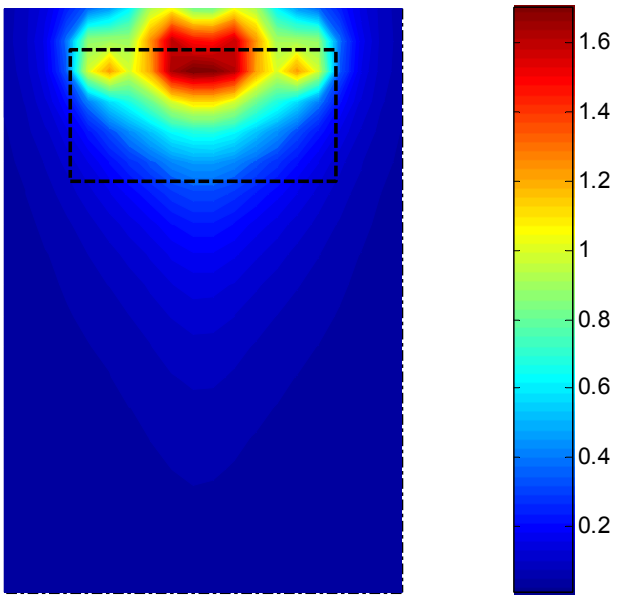

Figure 4.58 : Reconstruction associated with cascaded 4th order TLC for Example 4.3.2

Example 4.3.3 In the third example, two objects are buried under circular cross-sectional thin layer. One of the object is perfectly-conducting circle-shaped object with radius $0.4\lambda_0$ and other one is perfectly-conducting rectangle-shaped object with dimensions $\lambda_0 \times \lambda_0/2$. Relative permittivity of the thin layer is chosen as $\varepsilon_{r\,\delta} = 2.5 + 0.2i$. In this example, 240 sources are placed all around the cylindrical medium in free space. The other parameters are same as Example 4.3.1.

For this thickness ($\delta = 0.1\lambda_0$), the field and its normal derivative at the lower boundary of the thin layer are approximated with 2nd and 4th order thin layer conditions. Comparison of approximated and exact field and normal derivative of the field are given Figure 4.59 and Figure 4.60, respectively. It can be seen from Figure 4.59 and Figure 4.60, because of the small thickness of the layer, 2nd order condition is enough for approximation of fields.

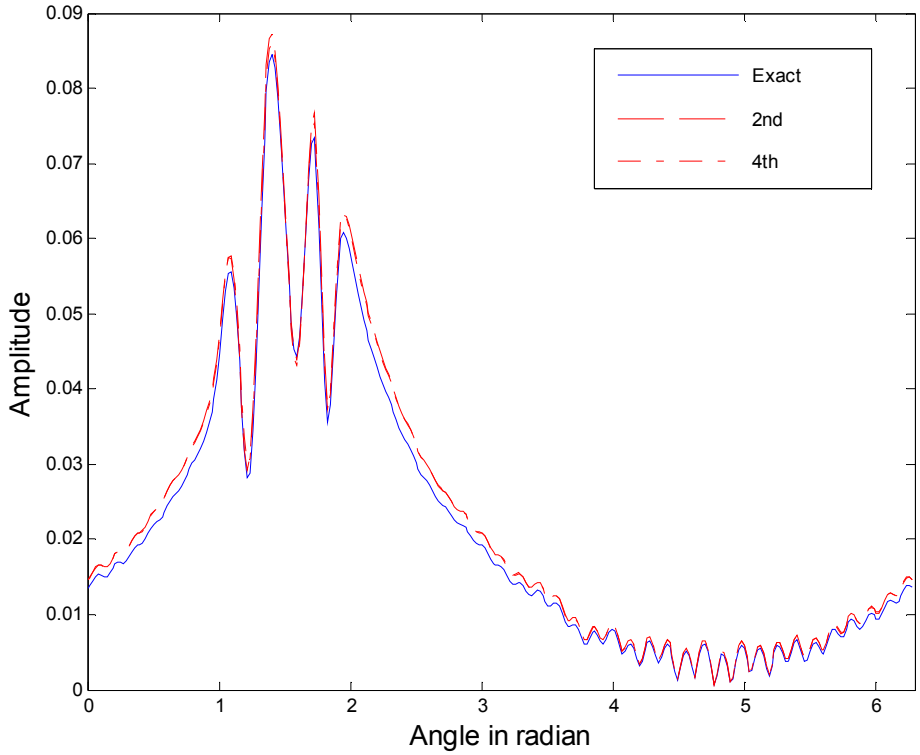

Figure 4.59 : Comparison of the fields at the lower boundary of the thin layer for Example 4.3.3

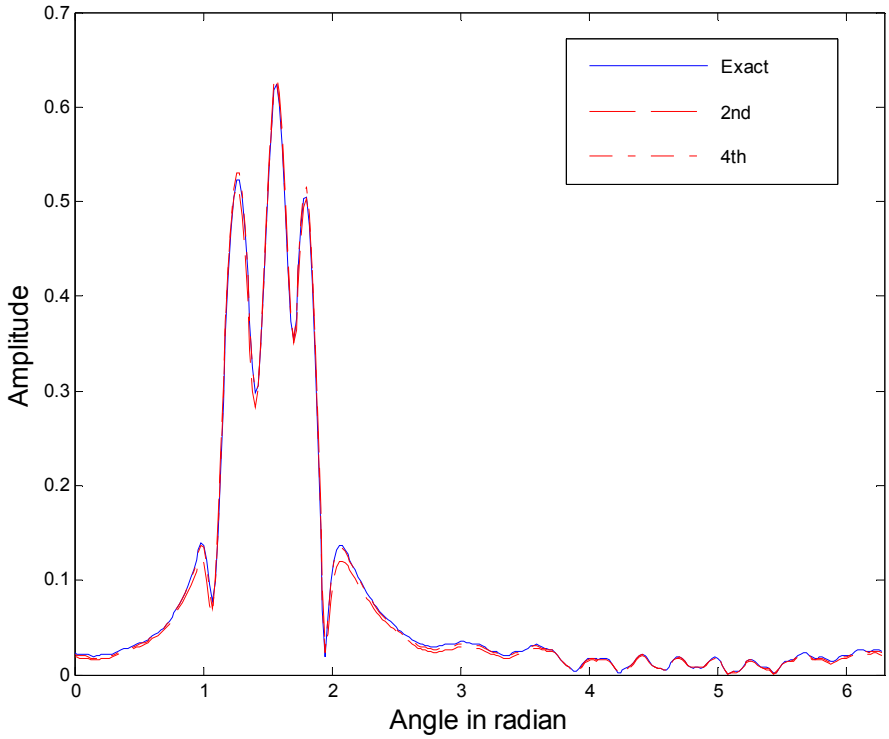

Figure 4.60 : Comparison of normal derivatives of the fields at the lower boundary of the thin layer for Example 4.3.3

Then, reconstructions of the object with exact data and data obtained by 2^{nd} and 4^{th} order TLC are done and presented in Figure 4.61, Figure 4.62 and Figure 4.63, respectively.

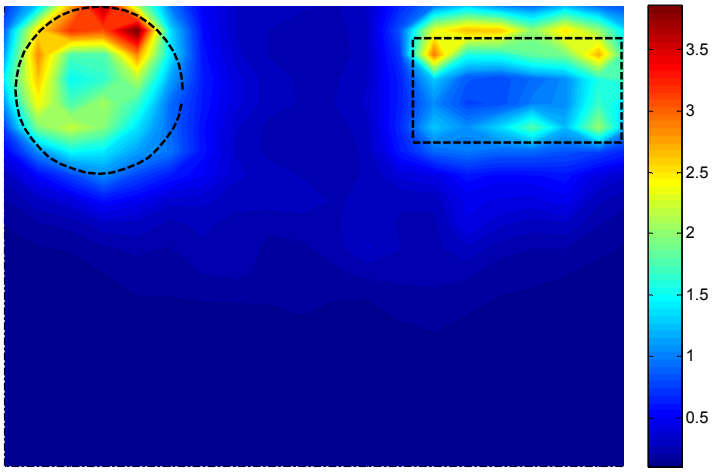

Figure 4.61 : Reconstruction associated with exact data for Example 4.3.3

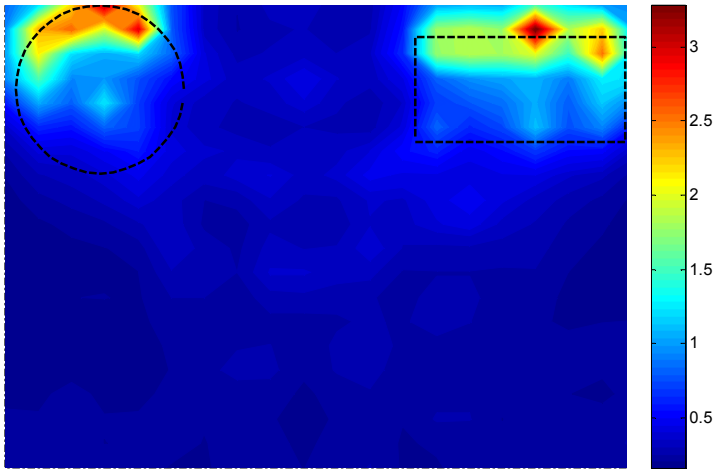

Figure 4.62 : Reconstruction associated with 2^{nd} order TLC for Example 4.3.3

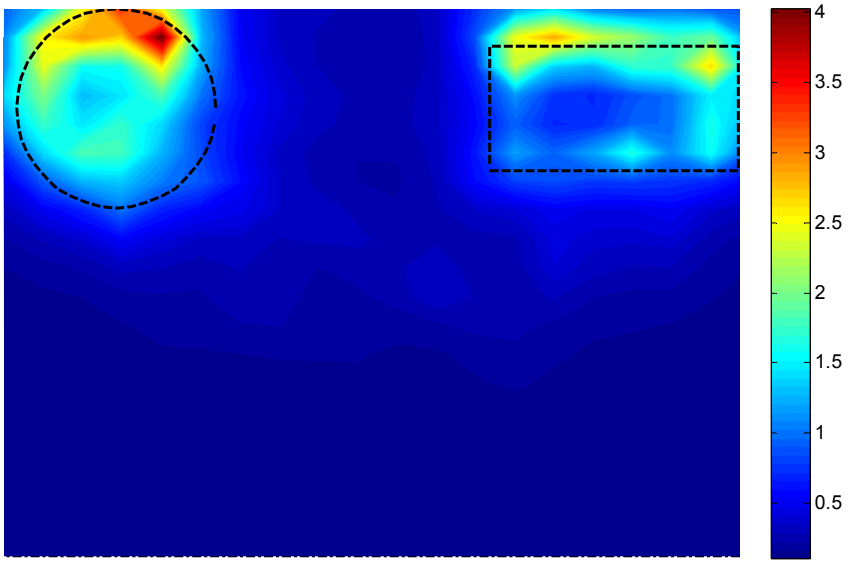

Figure 4.63 : Reconstruction associated with 4^{th} order TLC for Example 4.3.3

5. CONCLUSION

In this thesis, the use of thin layer conditions to reconstruct objects buried in a layered medium is investigated. At the first part the thesis, we have extended generalized thin layer conditions which link the field and its normal derivative on the lower boundary of the layer to the field and its normal derivative on the upper boundary of the layer. For this purpose, Helmholtz equation and boundary conditions are written in curvilinear coordinates and then field inside the thin layer is expanded into an asymptotic series in terms of its thickness. We have derived Thin Layer Conditions up to 4^{th} order.

In second part of the thesis, by the use of TLC, Reciprocity Gap Linear Sampling Method (RG-LSM) is applied to image objects buried under multilayered medium. RG-LSM needs to know field and its normal derivative on the boundary of the medium where object(s) is buried. To this aim, from the measurement data at the upper boundary, is converted to the data required by RG-LSM, by TLC.

At last part, numerical results are presented to show applicability of Thin Layer Conditions. We have shown that while 2^{nd} order TLC works for only small thickness and small permittivity, 4^{th} order TLC works for larger thickness and permittivity. Moreover, we have proposed Cascaded Thin Layer Conditions (C-TLC) in order to improve accuracy of approximations. The idea behind the C-TLC is to divide larger thickness into smaller ones and apply TLC for each one and cascade them. Since accuracy order of TLC is given by $O(\delta^k)$, better accuracy is obtained for the layers having smaller thickness and overall accuracy of C-TLC for original layer results in better than the one which TLC is applied only once to the original layer. In addition, we have presented numerical examples to show feasibility of TLC for any type of interface, i.e., flat and rough interfaced planar medium and also cylindrical medium.

REFERENCES

[1] **Senior, T.B.A. and Volakis, J.L.,** 1995. Approximate boundary conditions in electromagnetics, *IEE Electromagnetic Wave Series,* **41**

[2] **Duruflé, M., Haddar, H. and Joly, P.,** 2006. Higher order generalized impedance boundary conditions in electromagnetic scattering problems, *C.R. Physique*, **7**, pp. 533-542

[3] **Hoppe, D.J. and Rahmat-Samii, Y.,** 1992. Higher order impedance boundary conditions for anisotropic and nonreciprocal coatings, *IEEE Antennas and Propagation Society International Symposium,* **4**, pp. 1993-1996

[4] **Shumpert, J.D. and Senior, T.B.A.,** 2000. Impedance boundary conditions in ultrasonics, *IEEE Transactions on Antennas and Propagation,* **48 No 10**, pp. 1653-1659

[5] **Holloway, C.L. and Kuester, E.F.,** 1999. Effective boundary conditions for rough surfaces with a thin cover layer, *IEEE Antennas and Propagation Society International Symposium,* **1**, pp.506-509

[6] **Poirier, J.-R., Bendali, A. and Borderies, P.,** 2006. Impedance boundary conditions for the scattering of time-harmonic waves by rapidly varying surfaces, *IEEE Transactions on Antennas and Propagation,* **54 No 3**, pp. 995-1005

[7] **Mitzner, K.M.,** 1968. Effective boundary conditions for reflection and transmission by an absorbing shell of arbitrary shape, *IEEE Transactions on Antennas and Propagation,* **16**, pp. 706-712.

[8] **Karlsson, A.,** 2009. Approximate boundary conditions for thin structures, *IEEE Transactions on Antennas and Propagation,* **57 No 1**, pp. 144-148

[9] **Haddar, H. And Joly, P.,** 2002. Stability of thin layer approximation of electromagnetic waves scattering by linear and nonlinear coatings, *Journal of Computational&Applied Mathematics,* **143**, pp.201-236

[10] **Chun, S. and Hesthaven, J.S.,** 2009. High-order accurate thin layer approximations for time-domain electromagnetics and their implementation, Part I: Coatings, *Journal of Computational&Applied Mathematics*, **231**, pp.598-611

[11] **Chun, S., Haddar, H. and Hesthaven, J.S.,** 2010. High-order accurate thin layer approximations for time-domain electromagnetics, Part II: Transmission Layers, *Journal of Computational&Applied Mathematics.*

[12] **van den Berg, P.M. and Kleinman, R.E.,** 1997. A contrast source inversion method, *Inverse Problems,* **13**, pp. 1607-1620

[13] **Abubakar, A. and van den Berg, P.M.,** 2002. The contrast source inversion method for location and shape reconstructions, *Inverse Problems,* **18**, pp.495-510

[14] **Cui, T.J., Chew, W.C., Aydıner, A.A. and Chen S.,** 2001. Inverse scattering of two-dimensional dielectric objects buried in a lossy earth using the distorted born iterative method, *IEEE Transactions on Geoscience and Remote Sensing,* **39 No 2**, pp.339-346

[15] **Li, F., Liu, Q.H. and Song, L.P.,** 2004. Three-dimensional reconstruction of objects buried in layered media using Born and distorted Born iterative methods, *IEEE Geoscience and Remote Sensing Letters,* **1 No 2**, pp.107-111

[16] **Colton, D. and Kirsch A.,** 1996. A simple method for solving inverse scattering problems in the resonance region, *Inverse Problems*, **12**, pp. 383-393.

[17] **Catapano, I., Crocco, L. and Isernia, T.,** 2007. On simple methods for shape reconstruction of unknown scatterers, *IEEE Transactions on Antennas and Propagation,* **55 No 5**, pp.1431-1435.

[18] **Cakoni, F. and Colton, D.,** On the mathematical basis of the linear sampling method, *Georg. Math. J.*, **10**, pp. 911-925.

[19] **Arens, T.** 2004. Why linear sampling works, *Inverse Problems*, **20**, pp. 163-173.

[20] **Altuncu, Y., Akduman, İ. and Yapar, A.,** 2007. Detecting and locating dielectric objects buried under a rough interface, *IEEE Geoscience and Remote Sensing Letters,* **4 No 2**, pp.251-255

[21] **Lawrence, D. and Sarabandi K.,** 2002. Electromagnetic scattering from a dielectric cylinder buried beneath a slightly rough surface, *IEEE Transaction on Antennas and Propagation,* **50 No 10**

[22] **Tsang, L., Zhang, G. and Pak, K.,** 2002. Numerical study of detection of a buried object under a single random rough surface with angular correlation function, *IEEE Geoscience and Remote Sensing Symposium,* **4**, pp. 2143-2145

[23] **Sai, B. and Ligthart, L.P.,** 2003. Phase-based detection of small 3-D dielectric objects beneath rough surfaces, *2nd International Workshop on Advanced GPR,* pp.106-109

[24] **O'Neill, K.,** 2000. Broadband bistatic coherent and incoherent detection of buried objects beneath randomly rough surface, *IEEE Transactions on Geoscience and Remote Sensing,* **38 No 2**, pp.891-898

[25] **Tanaka, M., Takenaka, T., Harada, H. and Wall, D.J.N.,** 1994. An iterative inversion algorithm for the reconstruction of buried dielectric objects, *Antennas and Propagation Society International Symposium,* **3**, pp. 1640-1643

[26] **Chaturvedi, P. and Plumb, R.G.,** 1995. Electromagnetic imaging of underground targets using constrained optimization, *IEEE Transactions on Geoscience and Remote Sensing,* **33 No 3**, pp. 551-561

[27] **Feng, H., Castanon, D.A. and Karl, W.C.,** 1999. Underground imaging based on edge-preserving regularization, *IEEE International Conference on Information Intelligence and Systems,* pp.460-464

[28] **Baussard, A., Belkebir, K. and Premel, D.,** 2003. Regularized modified gradient method for inverse scattering problems, *IEEE Antennas and Propagation Society International Symposium,* **1**, pp.511-514

[29] **Colton, D. and Haddar, H.,** 2005. An application of the reciprocity gap functional to inverse scattering theory, *Inverse Problems*, **21**, pp. 383-398.

[30] **Cakoni, F., M'Barek, F. and Haddar, H.,** 2006. Analysis of two linear sampling methods applied to electromagnetic imaging of buried objects, *Inverse Problems,* **22**, pp.845-867

[31] **Delbary, F., Aramini, R., Bozza, G., Brignone, M. and Piana, M.,** 2008. On the use of the reciprocity gap functional in inverse scattering with near-field data : an application to mammography, *Journal of Physics,* **135**.

[32] **Cakoni, F. and Colton, D.,** 2006. Target identification of buried coated objects, *Journal of Computational&Applied Mathematics*, **25 No 2-3**, pp.269-288

APPENDIX

APPENDIX A.1: Solution procedure of 4th order thin layer approximation

To solve equations (2.68) and (2.69) in variational sense, auxiliary functions Φ_1 and Ψ_1 are written sum of basis functions with unknown coefficients, c_1 and d_1.

$$\Phi_1 = \sum c_{1j}\,\phi_j \qquad \textbf{(A.1.1)}$$

$$\Psi_1 = \sum d_{1j}\,\phi_j \qquad \textbf{(A.1.2)}$$

Then, we multiply both sides of equations (2.68) ,(2.69), (2.70) and (2.71) with roof top test function, we obtain followings

$$\int 2U^{+}\phi_i = 2\sum c_j \int \phi_j\phi_i + \delta \sum d_{1j} \int \phi_j\,\phi_i - \frac{\delta^3}{6}\sum d_j \int C^2\phi_j\phi_i$$

$$+\ \frac{\delta^3}{12}3\sum c_j \int \frac{\partial}{\partial s}\phi_j \frac{\partial}{\partial s}C\phi_i - \frac{\delta^3}{12}\sum c_j \left(\int Ck^2\,\phi_j\phi_i + \int C'\frac{\partial}{\partial s}\,\phi_j\phi_i\right) \qquad \textbf{(A.1.3)}$$

$$\int 2\frac{\partial U^{+}}{\partial n}\phi_i = 2\sum d_j \int \phi_j\phi_i - \delta \sum d_j \int C\,\phi_j\,\phi_i$$

$$+\frac{\delta^3}{12}\sum d_j \left(\int C'\phi_j \frac{\partial}{\partial s}\phi_i + \int 2k^2\mathrm{C}\phi_j\phi_i\right) + \frac{\delta^3}{12}\sum c_j \int C^2 \frac{\partial}{\partial s}\,\phi_j \frac{\partial}{\partial s}\,\phi_i$$

$$+\,\delta \sum c_{1j} \int \frac{\partial}{\partial s}\,\phi_j \frac{\partial}{\partial s}\phi_i - \delta k^2 \sum c_{1j} \int \phi_j\phi_i \qquad \textbf{(A.1.4)}$$

$$\sum d_{1j} \int \phi_j\phi_i + \sum d_{1j}\,\frac{\delta^2}{12}\int \frac{\partial}{\partial s}\phi_j \frac{\partial}{\partial s}\phi_i - \sum d_{1j}\,\frac{\delta^2 k^2}{12}\int \phi_j\phi_i = \sum d_j \int \phi_j\phi_i \qquad \textbf{(A.1.5)}$$

$$\sum c_{1j} \int \phi_j\phi_i + \sum c_{1j}\,\frac{\delta^2}{12}\int \frac{\partial}{\partial s}\phi_j \frac{\partial}{\partial s}\phi_i - \sum c_{1j}\,\frac{\delta^2 k^2}{12}\int \phi_j\phi_i = \sum c_j \int \phi_j\phi_i \qquad \textbf{(A.1.6)}$$

Finally, (A.1.3), (A.1.4), (A.1.5) and (A.1.6) are written in matrix form as:

$$\begin{bmatrix} H_{11} & H_{12} & H_{13} & H_{14} \\ H_{21} & H_{22} & H_{23} & H_{24} \\ H_{31} & H_{32} & H_{33} & H_{34} \\ H_{41} & H_{42} & H_{43} & H_{44} \end{bmatrix} \begin{bmatrix} C \\ D \\ C_1 \\ D_1 \end{bmatrix} = \begin{bmatrix} f_1 \\ f_2 \\ 0 \\ 0 \end{bmatrix} \qquad \textbf{(A.1.7)}$$

where $H_{11} = 2M_1 - \frac{\delta^3 k^2}{12} M_4 - \frac{\delta^3}{12} M_5 + \frac{\delta^3}{4} M_3$, $H_{12} = \frac{\delta^3}{6} M_2$, $H_{13} = \delta\ M_1$, $H_{21} = \frac{\delta^3}{12} M_7$, $H_{22} = 2M_1 - \delta M_4 + \frac{\delta^3}{12} M_8 - \frac{\delta^3 k^2}{6} M_4, H_{24} = \delta\ M_6 - \delta k^2 M_1$,

$H_{31} = -M_1$, $H_{33} = H_{44} = M_1 + \frac{\delta^2}{12} M_6 - \frac{\delta^2 k^2}{12} M_1$, $H_{31} = H_{42} = -M_1$, $H_{14} = H_{23} = H_{32} = H_{34} = H_{41} = H_{43} = 0$, $F_1 = \int 2U^+ \phi_i$, $F_2 = \int 2 \frac{\partial U^+}{\partial n} \phi_i$.

The terms in elements of matrix M_1, M_2 , M_3, M_4, M_5, M_6, M_7 and M_8 are defined as $\int \phi_j \phi_i$, $\int C^2 \phi_j \phi_i$, $\int \frac{\partial}{\partial s} \phi_j \frac{\partial}{\partial s} C \phi_i$, $\int C \phi_j \phi_i$, $\int C' \frac{\partial}{\partial s} \phi_j \phi_i$, $\int \frac{\partial}{\partial s} \phi_j \frac{\partial}{\partial s} \phi_i$, $\int C^2 \frac{\partial}{\partial s} \phi_j \frac{\partial}{\partial s} \phi_i$, $\int C' \phi_j \frac{\partial}{\partial s} \phi_i$, respectively.

We solve equation (A.1.7) to obtain unknown coefficients c, d, c_1 and d_1. And then using c, d, U^- and $\frac{\partial U^-}{\partial n}$ are obtained.

CURRICULUM VITAE

Candidate's full name: Alaaddin YAKA

Place and date of birth: Samsun, 09/11/1986

Permanent Address: Adalet Mah. Şehit Polis Serkan Yavuz Sokak No: 3/6
İlkadım/SAMSUN

Universities and Colleges attended: Istanbul Technical University,
Faculty of Electrical and Electronics Engineering,
Telecommunication Engineering, 2008.

Publications:

- Özdemir, Ö., Haddar, H., **Yaka, A.,** 2009: The Use of Thin Layer Conditions for the Reconstruction of Objects Buried in a Layered Medium. *PIERS Proceedings 2009,* pp.1808-1812, August 18-21, 2009 Moscow, Russia.